

REFINED TOPOLOGICAL VERTEX, CYLINDRIC PARTITIONS AND $U(1)$ ADJOINT THEORY

AMER IQBAL¹ CAN KOZÇAZ² KHURRAM SHABBIR³

¹ Department of Physics,
LUMS School of Science & Engineering,
U Block, D.H.A, Lahore, Pakistan.

² Department of Physics,
University of Washington,
Seattle, WA, 98195, U.S.A.

³ Abdus Salam School of Mathematical Sciences,
G. C. University,
Lahore, Pakistan.

Abstract

We study the partition function of the compactified 5D $U(1)$ gauge theory (in the Ω -background) with a single adjoint hypermultiplet, calculated using the refined topological vertex. We show that this partition function is an example a periodic Schur process and is a refinement of the generating function of cylindric plane partitions. The size of the cylinder is given by the mass of adjoint hypermultiplet and the parameters of the Ω -background. We also show that this partition function can be written as a trace of operators which are generalizations of vertex operators studied by Carlsson and Okounkov. In the last part of the paper we describe a way to obtain (q, t) identities using the refined topological vertex.

1 Introduction

The topological vertex formalism [1, 2] has not only been able to completely solve the problem of determining the Gromov-Witten/Gopakumar-Vafa/Donaldson-Thomas invariants of the toric Calabi-Yau threefolds but has also provided insights into their combinatorial aspects. In this paper we continue the study of the combinatorial aspects of the Nekrasov's extension of the topological string partition functions (which are same as the partition functions of the 5D compactified gauge theory in the Ω -background) for certain toric Calabi-Yau threefolds. Our main example will be a rather interesting Calabi-Yau threefold X_H which gives rise, via geometric engineering, to $U(1)$ gauge theory with one hypermultiplet in the adjoint representation. We provide a combinatorial interpretation of the refined partition function of X_H in terms of plane partitions living on a cylinder. These cylindric partitions were studied in [3] and are closely related with periodic Schur process. We will see that this cylinder naturally appears in the toric description of X_H and the size of the cylinder is determined by the mass of the adjoint hypermultiplet and the parameters (ϵ_1, ϵ_2) of the Ω -background. We only consider the $U(1)$ theory in this paper, however, the relation with periodic Schur process and cylindric partitions extends to the $U(N)$ theory with adjoint hypermultiplet as well [4].

The partition function of the 4D gauge theory was recently interpreted in terms of matrix elements of a vertex operator corresponding to certain K-theory classes on product of Hilbert schemes of \mathbb{C}^2 [5]. In this paper we make a similar attempt in trying to understand the compactified 5D gauge theory partition function in terms of certain (q, t) vertex operators which are a natural generalization of the vertex operators discussed in [5]. The relation with cylindric partitions implies that the matrix elements of these vertex operators are given by number of cylindric partitions of a certain type.

In the last section of the paper we derive a set of (q, t) identities associated with certain toric CY3-folds. These identities encode the fiber-base duality of the $\mathcal{N} = 2$ gauge theories [6].

The paper is organized as follows. In section 2 we give a detailed account of the refined vertex using the transfer matrix approach and give the refined crystal picture for the partition function of various CY3-folds. In section 3 we consider the partition function of $U(1)$ adjoint theory in detail and relate it to the combinatorics of cylindric plane partitions. We provide also provide an introduction to the basics of cylindric partitions. In section 4 we discuss the (q, t) generalization of the vertex operators of [5]. In section 5 we use the choice of the preferred direction needed for the refined vertex calculation to give a set of (q, t) identities associated with certain simple toric CY3-folds.

2 3D Partitions, Refined Vertex and Crystals

In this section, first we are going to review some background material including the definitions of 2D and 3D partitions, the partition function of a plane partition with multiple variables and the so-called transfer matrix approach to compute those partition functions. We should warn the reader that our presentation is going to be far from the most general form, but rather include only the special cases we need. Later, we are going to focus on the particular parametrization of the refined topological vertex and work out the crystal model for the closed refined topological vertex.

2.1 Transfer matrix approach

A 2D partition ν consists of non-negative integers with decreasing order $\nu = \{\nu_1 \geq \nu_2 \geq \dots, \nu_i \geq 0\}$. The pictorial representation obtained by placing ν_i boxes next to each other relates them to the Young diagrams. If we have another 2D partition λ in addition to ν such that $\lambda_i \geq \nu_i$ for all i we say λ includes ν and denote it by $\nu \subseteq \lambda$. This condition implies that any box (i, j) belonging to ν is also an element of λ . For two such partitions we can construct the skew partition λ/ν by removing all boxes that are elements of ν from λ , *i.e.*, $\lambda/\nu = \{(i, j) \in \lambda \mid (i, j) \notin \nu\}$. It is obvious from this definition that a skew partition might not be a partition. However, if λ is chosen to be $\lambda = \{\lambda_i = L \mid i = 1, \dots, M\}$ such that L and M are large enough to include ν in λ , the skew partition λ/ν is always a 2D partition.

A plane partition π is defined by an array of non-negative integers satisfying

$$\pi_{i,j} \geq \pi_{i+r,j+s}, \quad r, s \geq 0. \quad (2.1)$$

Plane partitions have also a 3-dimensional pictorial representation: if we divide the base xy -plane into unit squares and denote them by (i, j) , we can place $\pi_{i,j}$ boxes over each square (i, j) . In this sense, plane partitions are considered a generalization of Young diagrams. The total number of boxes of a plane partition π is given by

$$|\pi| = \sum_{i,j} \pi_{i,j}.$$

A skew 3D partition of shape λ/ν is an array of non-negative integers $\{\pi_{i,j} \mid (i, j) \in \lambda/\nu\}$ satisfying the same condition as in Eq. (2.1).

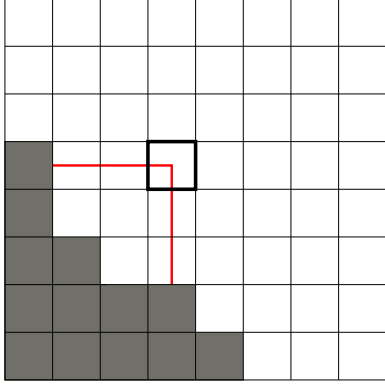


Figure 1: The hook length of a box in ν^c .

The partition function corresponding to a skew plane partition of shape ν^c (the complement of ν) is given by

$$\begin{aligned} Z_\nu(q) &:= \sum_{\pi(\nu^c)} q^{|\pi|} \\ &= \prod_{(i,j) \in \nu^c} \frac{1}{1 - q^{\hat{h}(i,j)}}, \end{aligned} \quad (2.2)$$

where $\hat{h} = j - \nu_i + i - \nu_j^t - 1$ is the hook length of the box $(i, j) \in \nu^c$ as shown in Fig. 1.

If ν is the empty partition \emptyset , the partition function becomes the MacMahon function,

$$M(q) := Z_\emptyset(q) = \prod_{k=1}^{\infty} \frac{1}{(1 - q^k)^k}. \quad (2.3)$$

If we normalize the partition function $Z_\nu(q)$ by the MacMahon function $M(q)$ then we obtain $\tilde{Z}_\nu(q)$ given by

$$\tilde{Z}_\nu(q) := \frac{Z_\nu(q)}{M(q)} = \prod_{(i,j) \in \nu} \frac{1}{1 - q^{h(i,j)}}, \quad (2.4)$$

where $h(i, j) = \nu_i - j + \nu_j^t - i + 1$ is the hook length of a box in ν . This partition function as well as more general ones which we will define shortly can be computed using transfer matrix formalism. We can consider a plane partition function as a sequence of 2D partitions, $\{\eta(a) | a \in \mathbb{Z}\}$, along the slices whose projection to the base is given by $y - x = a$.

This sequence is obtained by slicing the plane partition by diagonal planes as shown in Fig. 2. The definition of a plane partition puts strong conditions among the 2D partitions in the sequence. Before we spell out these conditions we need to define *interlacing*: we say a 2D partition μ interlaces another 2D partition ν , written as $\mu \succ \nu$, if

$$\mu_1 \geq \nu_1 \geq \mu_2 \geq \nu_2 \geq \dots \quad (2.5)$$

Note that interlacing is a stronger condition than including. The diagonal slices $\eta(a)$ obtained from a plane partition satisfy

$$\begin{aligned} \eta(a+1) &\succ \eta(a), & a < 0, \\ \eta(a) &\succ \eta(a+1), & a \geq 0. \end{aligned} \quad (2.6)$$

Now we are ready to define, following [7], a more generalized partition function of a plane partition: we can weigh different slices of the 3D partition with different variables, hence the partition function becomes

$$Z_\nu(\{q_a\}) := \sum_{\{\eta(a)\}} \prod_{a \in \mathbb{Z}} q_a^{|\eta(a)|} = \sum_{\pi} \prod_{a \in \mathbb{Z}} q_a^{|\pi_a|} \quad (2.7)$$

where $|\pi_a| = \sum_i \pi_{i, a+i}$. It is obvious from this definition that we will obtain the partition function we previously defined if we set all variables equal to each other, $\{q_a = q\}$.

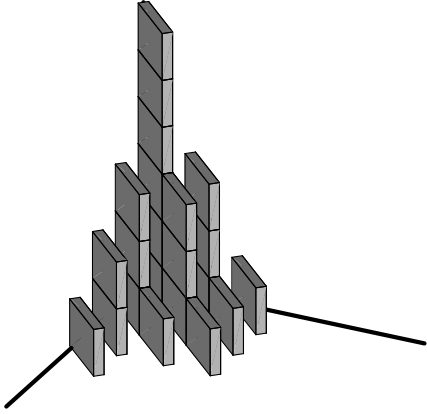


Figure 2: The diagonal slicing of the plane partition.

The transfer matrix approach is based on associating a fermionic Fock space to 2D partitions. We will introduce creation/annihilation as well as the so-called vertex operators acting on this space of states equipped with a natural inner product.

The Fock space \mathcal{F} is a semi-infinite product of another vector space V spanned by vectors \underline{k} , where $k \in \mathbb{Z} + 1/2$. An element v_S of the Fock space $\mathcal{F} = \bigwedge^{\infty} V$ is given by

$$v_S = \underline{s_1} \wedge \underline{s_2} \wedge \underline{s_3} \wedge \dots, \quad (2.8)$$

where $S = s_1 > s_2 > \dots$ is a subset of $\mathbb{Z} + 1/2$, such that $S \setminus (\mathbb{Z}_{\leq 0} - 1/2)$ and $(\mathbb{Z}_{\leq 0} - 1/2) \setminus S$ are both finite. Over this space there is a natural inner product with respect to which the basis defined by $\{v_S\}$ is orthonormal.

The generators ψ_k and ψ_k^* of Clifford algebra satisfy the following anti-commutation relations:

$$\{\psi_k, \psi_{k'}\} = 0, \quad \{\psi_k^*, \psi_{k'}^*\} = 0, \quad \{\psi_k, \psi_{k'}^*\} = \delta_{kk'}, \quad (2.9)$$

where $k, k' \in \mathbb{Z} + 1/2$. Later we will need the explicit action of the Clifford algebra generators on the basis vectors

$$\psi_k (\underline{s_1} \wedge \underline{s_2} \wedge \underline{s_3} \wedge \dots) = \underline{k} \wedge \underline{s_1} \wedge \underline{s_2} \wedge \underline{s_3} \wedge \dots \quad (2.10)$$

$$\psi_k^* (\underline{s_1} \wedge \underline{s_2} \wedge \dots \wedge \underline{s_l} \wedge \underline{k} \wedge \underline{s_{l+1}} \wedge \dots) = (-1)^l \underline{s_1} \wedge \underline{s_2} \wedge \dots \wedge \underline{s_l} \wedge \underline{s_{l+1}} \wedge \dots \quad (2.11)$$

$$\psi_k^* (\underline{s_1} \wedge \underline{s_2} \wedge \underline{s_3} \wedge \dots) = 0, \quad \text{for } k \in \mathbb{Z} \setminus S. \quad (2.12)$$

The vectors in the Fock space \mathcal{F} can be parameterized by partitions:

$$v_\lambda^{(0)} = \underline{\lambda_1 - 1/2} \wedge \underline{\lambda_2 - 3/2} \wedge \dots \quad (2.13)$$

where we ignore an irrelevant shift m of the vacuum energy from the definition in [7]. In our notation, $v_0^{(0)}$ denotes the vacuum state corresponding to empty partition \emptyset .

At this point, we have constructed a fermionic Fock space with Clifford algebra acting on it and established one-to-one correspondence with the 2D partition. What is needed to continue is an operator which can create states corresponding to 2D partitions which interlace a given 2D partition after acting on a given state. To construct this operator first we need to define α_n

$$\alpha_n = \sum_{k \in \mathbb{Z} + 1/2} \psi_{k+n} \psi_k^*, \quad n = \pm 1, \pm 2, \dots \quad (2.14)$$

These operators satisfy the following commutation relationships:

$$[\alpha_n, \alpha_m] = -n\delta_{n,-m}, \quad [\alpha_n, \psi_k] = \psi_{k+n}, \quad [\alpha_n, \psi_k^*] = -\psi_{k-n}^*. \quad (2.15)$$

The vertex operators are obtained from these operators α_n 's by exponentiation

$$\Gamma_+(x) = \exp\left(\sum_{n \geq 1} \frac{x^n}{n} \alpha_n\right), \quad (2.16)$$

$$\Gamma_-(x) = \exp\left(\sum_{n \geq 1} \frac{x^n}{n} \alpha_{-n}\right). \quad (2.17)$$

$\Gamma_+(x)$ and $\Gamma_-(x)$ are conjugates of each other with respect to the inner product on \mathcal{F} :

$$(\Gamma_-(x)v, w) = (v, \Gamma_+(x)w). \quad (2.18)$$

The action of $\Gamma_-(x)$ on the vacuum state is particularly important, $\Gamma_-(x)v_0^{(0)} = v_0^{(0)}$. It is easy to verify that they satisfy the following commutation relation which we are going to use extensively (in addition to its action on the vacuum state as well as the conjugacy property):

$$\Gamma_+(x)\Gamma_-(y) = (1 - xy)\Gamma_-(y)\Gamma_+(x). \quad (2.19)$$

Let us discuss this formal construction a little bit more explicitly. For the simplest cases, one can easily convince oneself of the above relation by expanding the exponential in $\Gamma_+(x)$ as a power series and acting with the individual terms in the expansion on a given state. One creates a generating function for all partitions that interlace the one acted on. This is summarized as

$$\prod_i \Gamma_+(x_i) v_\mu^{(0)} = \sum_{\lambda \supset \mu} s_{\lambda/\mu}(x) v_\lambda^{(0)}. \quad (2.20)$$

More specifically

$$\Gamma_+(1)v_\mu^{(0)} = \sum_{\lambda \supset \mu} v_\lambda^{(0)}, \quad (2.21)$$

since $s_{\lambda/\mu}(1) = 1$ if $\lambda \succ \mu$, and vanishes otherwise.

The generalized partition function can be written in terms of the vertex operators. To sum over all possible plane partitions, one way is to start at $a = \infty$ with vacuum and apply $\Gamma_+(x)$. We end up with all possible partitions as a generating function on the next slice that interlace vacuum. Then we successively apply $\Gamma_+(x)$ until we hit the main diagonal slice $a = 0$. This way, we create partitions which interlace the partitions on the previous slice. After the main diagonal we start applying $\Gamma_-(y)$'s successively, and we create partitions that are interlaced by the previous slices, until we reach at $a = -\infty$. The transfer matrix formalism can be used in a more general situation when we asymptotically have non-trivial states at $a = \pm\infty$.

The partition function of a skew 3D partition depends on the 2D partition ν on the base. We divide the corners of the corresponding 2D partition into *inner* and *outer* corners. We parameterize the inner and outer corners by their coordinates v_i and u_i , respectively, of their projection onto the real line as shown in Fig. 3. It is convenient to introduce another set of parameters $\{x_m^\pm | m \in \mathbb{Z} + 1/2\}$ and identify them with q_a 's in the following shape dependent way [7]:

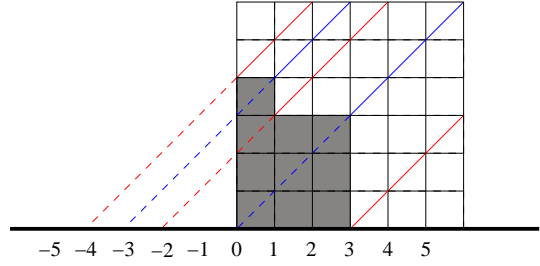


Figure 3: Three inner corners $\{v_1, v_2, v_3\} = \{-4, -2, 3\}$, two outer corners $\{u_1, u_2\} = \{-3, 0\}$.

$$\begin{aligned}
\frac{x_{m+1}^+}{x_m^+} &= q_{m+\frac{1}{2}}, \quad m > v_M \text{ or } u_i - 1 > m > v_i, \\
x_{u_i-\frac{1}{2}}^+ x_{u_i+\frac{1}{2}}^- &= q_{u_i}^{-1}, \\
x_{v_i-\frac{1}{2}}^- x_{v_i+\frac{1}{2}}^+ &= q_{v_i}, \\
\frac{x_m^-}{x_{m+1}^-} &= q_{m+\frac{1}{2}}, \quad m < v_1 \text{ or } v_{i+1} - 1 > m > u_i,
\end{aligned} \tag{2.22}$$

where M is the number of outer corners. In terms of these new variables, the generalized partition function reads

$$\begin{aligned}
Z_\nu(\{x_m^\pm\}) &= \left(\prod_{u_M > m > v_M} \Gamma_-(x_m^+) \dots \prod_{u_i < m < v_{i+1}} \Gamma_+(x_m^-) \prod_{v_i < m < u_i} \Gamma_-(x_m^+) \dots \right. \\
&\quad \left. \prod_{v_1 > m > u_0} \Gamma_+(x_m^-) v_0^{(0)}, v_0^{(0)} \right) = \left(\prod_{u_0 < m < u_N} \Gamma_{-\varepsilon(m)}(x_m^{\varepsilon(m)}) v_0^{(0)}, v_0^{(0)} \right),
\end{aligned} \tag{2.23}$$

where m runs over $\mathbb{Z}+1/2$. In the last equation, we have introduced some new notation; $\varepsilon(m) = +$, if $v_i < m < u_i$ for $1 \leq i \leq M$ and, $\varepsilon(m) = -$, if $u_i < m < v_{i+1}$ for $0 \leq i \leq M - 1$. This partition function turns out to have a nice compact form [7]

$$Z_\nu(\{x_m^\pm\}) = \prod_{\substack{m_1 < m_2 \\ m_1 \in D^-, m_2 \in D^+}} (1 - x_{m_1}^- x_{m_2}^+)^{-1}, \quad (2.24)$$

with $D^\pm = \{m \mid \varepsilon(m) = \pm\}$.

2.2 Refined topological vertex

The transfer matrix formalism reviewed in the last section is capable of computing a partition function with infinitely many parameters, one for each diagonal slice. However, the main motivation to construct a more refined topological vertex comes from the microscopic derivation of the Seiberg-Witten solution [8], and it has only two distinct parameters, q and t . We will review the correct choice of assigning equivariant parameters to the diagonal slices, *i.e.*, the map $\{q_a \mid a \in \mathbb{Z}\} \mapsto \{q, t\}$. We will refer the interested reader to the original reference [9] for the details of the physical motivation as well as the derivation of the refined topological vertex. Here, we only give the map.

Imagine we are computing the partition function Z_ν for a partition ν shown in Fig. 4. According the transfer matrix method we have a series of diagonal slices presented by the red and blue lines in the figure. As we mentioned before we start at $a = \infty$ and apply Γ_\pm repeatedly, following the arrows. For each partition we can construct a “barcode” by assigning a black or white box depending on whether we are going horizontally or vertically, respectively, while we are tracing the profile of ν . Note that if we count the number of black boxes to the left of the i^{th} white box, we get ν_i . For example, there are 5 black boxes to the left of the first white box. Similarly, if we count the number of white boxes to the right of the j^{th} black box, we obtain ν_j^t . It turns out that this barcode is in one-to-one correspondence with 2D partitions. The (q, t) -assignment to each slice is essentially determined by this barcode, whenever we go vertically we count that slice with q , otherwise, along each horizontal pass, with t . For an

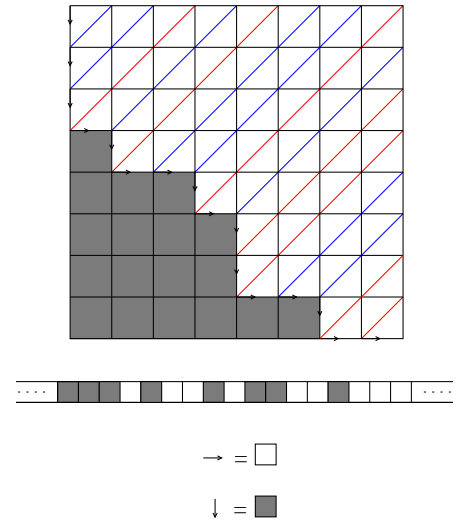


Figure 4: The parameters q and t are assigned based on the partition $\nu = (5, 4, 4, 3, 1, 1)$.

arbitrary 2D partition ν the map has the following form:

$$\{x_m^+ | m \in D^+\} = \{t^i q^{-\nu_i} | i = 1, 2, 3, \dots\}, \quad (2.25)$$

$$\{x_m^- | m \in D^-\} = \{q^{j-1} t^{-\nu_j^t} | j = 1, 2, 3, \dots\}. \quad (2.26)$$

In general, at the asymptotes $a = \pm\infty$, we may not have empty partitions but instead two different partitions, say λ and μ . The interlacing condition Eq. (2.6) requires us to excise the whole region behind those two partitions. In this sense, we are computing the transition from a 2D partition λ to another one μ . This is the generating function of all possible 3D partitions we can create by putting boxes in the empty region left by excising the three asymptotes [10],

$$Z_{\lambda\mu\nu}(t, q) := \left(\prod_{u_0 < m < u_N} \Gamma_{-\varepsilon(m)}(x_m^{\varepsilon(m)}) v_\lambda^{(0)}, v_\mu^{(0)} \right). \quad (2.27)$$

The refined topological vertex is then defined to be

$$\begin{aligned} C_{\lambda\mu\nu}(t, q) &= \frac{Z_{\lambda\mu\nu}(t, q)}{Z_{\emptyset\emptyset\emptyset}(t, q)} \\ &= \left(\frac{q}{t}\right)^{\frac{\|\mu\|^2 + \|\nu\|^2}{2}} t^{\frac{\kappa(\mu)}{2}} P_{\nu^t}(t^{-\rho}; q, t) \sum_{\eta} \left(\frac{q}{t}\right)^{\frac{|\eta| + |\lambda| - |\mu|}{2}} s_{\lambda^t/\eta}(t^{-\rho} q^{-\nu}) s_{\mu/\eta}(t^{-\nu^t} q^{-\rho}), \end{aligned} \quad (2.28)$$

where

$$\begin{aligned} P_{\nu^t}(t^{-\rho}; q, t) &= t^{\frac{\|\nu\|^2}{2}} \tilde{Z}_\nu(t, q) \\ &= t^{\frac{\|\nu\|^2}{2}} \prod_{(i,j) \in \nu} \left(1 - t^{a(i,j)+1} q^{\ell(i,j)}\right)^{-1}, \quad a(i, j) = \nu_j^t - i, \quad \ell(i, j) = \nu_i - j. \end{aligned}$$

2.3 Crystal models and (t, q) parameters

In this section, we will discuss crystal models for $X_0 := \mathcal{O}(-1) \oplus \mathcal{O}(-1) \mapsto \mathbb{P}^1$ and $X_1 := \mathcal{O}(0) \oplus \mathcal{O}(-2) \mapsto \mathbb{P}^1$. We will see that both these models have exactly the same combinatorial description with the only difference being the expansion parameters. A better understanding of these combinatorial models and the expansion parameters (q, t) will help us later understand the combinatorial model for the compactified resolved conifold which gives rise to $U(1)$ gauge theory with adjoint matter.

Recall that the refined partition function of X_0 and X_1 is given by [9] (this can be calculated using

the topological vertex formalism)¹

$$Z_{X_0}(Q, t, q) = \prod_{i,j=1}^{\infty} \left(1 - Q t^{i-\frac{1}{2}} q^{j-\frac{1}{2}}\right), \quad Z_{X_1}(Q, t, q) = \prod_{i,j=1}^{\infty} \left(1 - Q t^i q^{j-1}\right)^{-1}. \quad (2.32)$$

Where $T = -\log(Q)$ is the Kähler parameter associated with the \mathbb{P}^1 in the geometry. The combinatorial interpretation of $Z_{X_1}(Q, q, q)$ in terms of 3D partitions is well known [?]. A similar combinatorial interpretation for $Z_{X_1}(Q, t, q)$ can be found: Given a 3D partition π and its diagonal slices $\{\eta(a), a \in \mathbb{Z}\}$

$$\begin{aligned} \sum_{\pi, \eta(0)=\lambda} q^{\sum_{a>0} |\eta(a)|} t^{\sum_{a \leq 0} |\eta(a)|} &= t^{\sum_i i \lambda_i} q^{\sum_i (i-1) \lambda_i} \prod_{s \in \lambda} \left(1 - q^{h(s)}\right)^{-1} \left(1 - t^{h(s)}\right)^{-1} \\ &= s_{\lambda}(t, t^2, t^3, \dots) s_{\lambda}(1, q, q^2, \dots). \end{aligned} \quad (2.33)$$

The prefactor $t^{\sum_i i \lambda_i} q^{\sum_i (i-1) \lambda_i}$ arises because if $\eta(0) = \lambda$ then the 3D partition with the least number of boxes is such that there are $\sum_i i \lambda_i$ number of boxes on or to the right of the main

¹The refined topological string partition function in terms of Gopakumar-Vafa invariants can be written as

$$Z_X(\omega, t, q) := \prod_{C \in H_2(X, \mathbb{Z})} \prod_{j_L, j_R} \prod_{k_L = -j_L}^{j_L} \prod_{k_R = -j_R}^{j_R} \prod_{m_1, m_2=1}^{\infty} \left(1 - t^{k_L + k_R + m_1 - \frac{1}{2}} q^{k_L - k_R + m_2 - \frac{1}{2}} e^{-\omega \cdot C}\right)^{(-1)^{2(j_L + j_R)} N_C^{j_L, j_R}(X)}.$$

For the case of X_0 and X_1 this simplifies to

$$Z_{X_k}(Q, t, q) = \prod_{j_L, j_R} \prod_{k_L = -j_L}^{j_L} \prod_{k_R = -j_R}^{j_R} \prod_{m_1, m_2=1}^{\infty} \left(1 - t^{k_L + k_R + m_1 - \frac{1}{2}} q^{k_L - k_R + m_2 - \frac{1}{2}} Q\right)^{(-1)^{2(j_L + j_R)} N_C^{j_L, j_R}(X_k)}. \quad (2.29)$$

For X_0 the moduli space of \mathbb{P}^1 is just a point therefore $N_C^{j_L, j_R} = \delta_{j_L, 0} \delta_{j_R, 0}$. For X_1 the moduli space of \mathbb{P}^1 is \mathbb{C} . If the moduli space had been \mathbb{P}^1 this would have given the spin content $(j_L, j_R) = (0, \frac{1}{2}) \Rightarrow (k_L, k_R) = (0, \{-\frac{1}{2}, +\frac{1}{2}\})$. Since the moduli space is \mathbb{C} we can think of it as half- \mathbb{P}^1 giving the spin content $(j_L, j_R) = (0, \frac{1}{2}) \Rightarrow (k_L, k_R) = (0, \{+\frac{1}{2}\})$. Thus we get

$$Z_{X_0}(Q, t, q) = \prod_{i,j=1}^{\infty} \left(1 - Q t^{i-\frac{1}{2}} q^{j-\frac{1}{2}}\right), \quad Z_{X_1}(Q, t, q) = \prod_{i,j=1}^{\infty} \left(1 - Q t^i q^{j-1}\right)^{-1}. \quad (2.30)$$

Of course, we could choose the spin content for half- \mathbb{P}^1 to be $(j_L, j_R) = (0, \frac{1}{2}) \Rightarrow (k_L, k_R) = (0, \{-\frac{1}{2}\})$. In this case we get

$$Z_{X_1}(Q, t, q) = \prod_{i,j=1}^{\infty} \left(1 - Q t^{i-1} q^j\right)^{-1}. \quad (2.31)$$

In terms of combinatorics of 3D partitions the two choices for the spin content correspond to the choice of counting the partition $\eta(0)$ (the 2D partition on the main diagonal) with t or q .

diagonal and $\sum_i (i-1)\lambda_i$ is the number of boxes below the diagonal. Thus

$$\begin{aligned} \sum_{\lambda} Q^{|\lambda|} \sum_{\pi, \eta(0)=\lambda} q^{\sum_{a>0} |\eta(a)|} t^{\sum_{a\leq 0} |\eta(a)|} &= \sum_{\lambda} Q^{|\lambda|} s_{\lambda}(t, t^2, \dots) s_{\lambda}(1, q, \dots) \\ &= \prod_{i,j=1}^{\infty} (1 - Q t^i q^{j-1})^{-1} = Z_{X_1}(Q, t, q). \end{aligned}$$

The refined partition function $Z_{X_0}(Q, t, q)$ has a similar combinatorial description in which instead of counting the slices with parameters q and t we count them with q and t^{-1} and also splitting the slice $\eta(0)$ symmetrically between the two parameters,

$$\begin{aligned} \sum_{\lambda} Q^{|\lambda|} \sum_{\pi, \eta(0)=\lambda} q^{\frac{|\eta(0)|}{2} + \sum_{a>0} |\eta(a)|} (t^{-1})^{\frac{|\eta(0)|}{2} + \sum_{a<0} |\eta(a)|} &= \sum_{\lambda} Q^{|\lambda|} s_{\lambda}(t^{-\frac{1}{2}}, t^{-\frac{3}{2}}, \dots) s_{\lambda}(q^{\frac{1}{2}}, q^{\frac{3}{2}}, \dots) \\ &= \sum_{\lambda} Q^{|\lambda|} (-1)^{|\lambda|} s_{\lambda t}(t^{\frac{1}{2}}, t^{\frac{3}{2}}, \dots) s_{\lambda}(q^{\frac{1}{2}}, q^{\frac{3}{2}}, \dots) = \prod_{i,j=1}^{\infty} (1 - Q t^{i-\frac{1}{2}} q^{j-\frac{1}{2}}) = Z_{X_0}(Q, t, q). \end{aligned}$$

Thus we see that both $Z_{X_0}(Q, t, q)$ and $Z_{X_1}(Q, t, q)$ can be expressed as a sum over 3D partitions as long as correct expansion parameters are chosen.

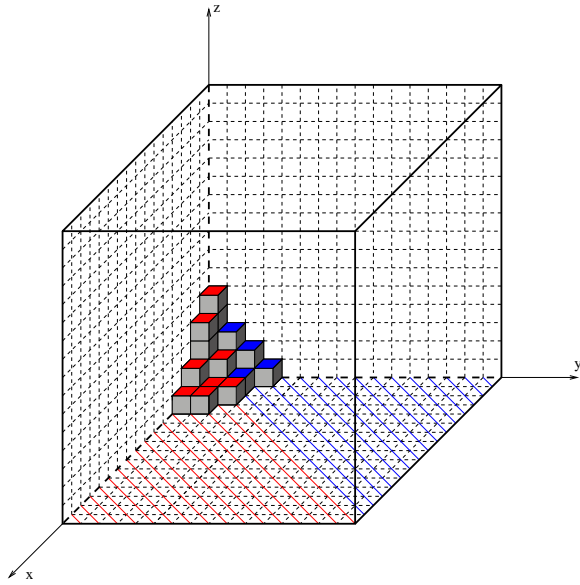


Figure 5: 3D partition and choice of slicing.

The location of this second wall is related to the appropriate Kähler parameter in the toric geometry. Later, for the closed refined topological vertex, we will introduce a projection operator and put a “ceiling” in the region where we grow the crystal, that is equivalent putting a last wall parallel to the xy -plane.

The above is not the only crystal model for $Z_{X_0}(Q, q, q)$. Another model in terms 3D partitions has been discussed [11]. The model consists of putting an additional “wall” parallel to one of the already existing walls bounding the positive octant \mathbb{R}^{3+} , say the one along the xz -plane, in the region where we are growing our crystal. The distance of this additional wall to xz -plane is related to the Kähler parameter of the resolved conifold. The region bounded by these walls seems like the toric diagram of the resolved conifold. Later we will consider the double- \mathbb{P}^1 and the closed topological vertex for the refined case. First, we will allow the size of the preferred direction to be non-compact. This is equivalent to placing another wall, now parallel to the yz -plane, and allowing the crystal grow in the z -direction without any bound. Again, the

In Fig. 5, we show an example of a plane partition and show how the slices should be weighted; each blue slice, *i.e.* $a > 0$, gives rise to a factor of $q^{|\eta(a)|}$, whereas each red slice contributes $t^{|\eta(a)|}$ with $a \leq 0$. For instance, the 3D partition in the figure counts as $q^7 t^{17}$.

The refined partition function of X_0 can also be obtained by putting a wall at a distance of M along the y -direction. The partition function reads then

$$Z_{\text{crystal}} = \left(\prod_{\infty > m > 0} \Gamma_-(x_m^+) \prod_{0 > m > -M} \Gamma_+(x_m^-) v_0^{(0)}, v_0^{(0)} \right). \quad (2.34)$$

We can repeatedly make use of the commutation relation Eq.(2.19) of the vertex operators to get

$$Z_{\text{crystal}} = \prod_{k_1=1}^{\infty} \prod_{k_2=1}^M \left(1 - x_{k_1-1/2}^+ x_{-k_2+1/2}^- \right)^{-1} \underbrace{\left(\prod_{0 > m > -M} \Gamma_+(x_m^-) \prod_{\infty > m > 0} \Gamma_-(x_m^+) v_0^{(0)}, v_0^{(0)} \right)}_{=1} \quad (2.35)$$

and then it is easy to see that the inner product is equal to 1, due to the Eq. (2.18) and the fact that $\Gamma_-(x_m^+)$ acts as identity on the vacuum state $v_0^{(0)}$. We have already established the map between $\{q, t\}$ and $\{x_m^{\pm}\}$ in Eq. (2.25), the partition function from the 3D crystal takes the form

$$Z_{\text{crystal}} = \prod_{i=1}^{\infty} \prod_{j=1}^M (1 - t^i q^{j-1})^{-1}. \quad (2.36)$$

Since

$$Z_{X_0}(Q, t, q) = \prod_{i=1}^{\infty} \prod_{j=1}^{\infty} \left(1 - Q t^{i-\frac{1}{2}} q^{j-\frac{1}{2}} \right), \quad (2.37)$$

these two partition functions turn out to be related to each other in the same way as in [12]:

$$Z_{\text{crystal}} = M(t, q) Z_{X_0}(Q, t, q), \quad (2.38)$$

with the identification $Q \sqrt{\frac{q}{t}} = q^M$. $M(t, q)$ is the refined MacMahon function already defined in [9]:

$$M(t, q) = \prod_{i=1}^{\infty} \prod_{j=1}^{\infty} (1 - t^i q^{j-1})^{-1}. \quad (2.39)$$

2.3.1 Double- \mathbb{P}^1 and closed refined topological vertex

In this section, we will first place the second wall in our crystal and then put the ceiling. While introducing the second wall is in the same spirit as placing the first wall, the ceiling will require, as mentioned, the introduction of a projection operator \mathcal{P}_N .

In Fig. 6 we have the toric diagram for the double- \mathbb{P}^1 . The double blue lines show our choice of the preferred direction. The crystal partition function is given by

$$Z_{\text{crystal}} = \left(\prod_{L>m>0} \Gamma_-(x_m^+) \prod_{0>m>-M} \Gamma_+(x_m^-) v_0^{(0)}, v_0^{(0)} \right) \quad (2.40)$$

We repeat the same steps as in the previous example and obtain

$$Z_{\text{crystal}} = \prod_{i=1}^L \prod_{j=1}^M (1 - t^i q^{j-1})^{-1}. \quad (2.41)$$

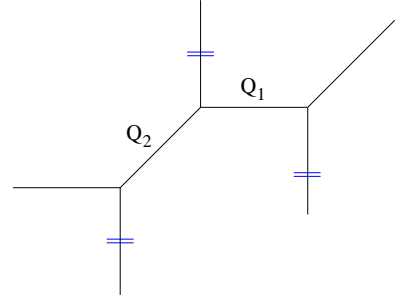


Figure 6: Toric diagram of double- \mathbb{P}^1 .

The refined vertex computation (see Appendix A) gives

$$Z_{\text{double } \mathbb{P}^1}(Q_1, Q_2, t, q) = \prod_{i=1}^{\infty} \prod_{j=1}^{\infty} \frac{(1 - Q_1 t^{i-\frac{1}{2}} q^{j-\frac{1}{2}})(1 - Q_2 t^{i-\frac{1}{2}} q^{j-\frac{1}{2}})}{(1 - Q_1 Q_2 t^{i-1} q^j)}. \quad (2.42)$$

After the following identification

$$Q_1 \sqrt{\frac{q}{t}} = q^M, \quad Q_2 \sqrt{\frac{q}{t}} = t^L,$$

we get

$$Z_{\text{crystal}} = M(t, q) Z_{\text{double } \mathbb{P}^1}(Q_1, Q_2, t, q). \quad (2.43)$$

Let us now introduce the projection operator we mentioned before. The goal for such an operator is to eliminate the contributions coming from the 3D partition which are higher than our ‘‘ceiling’’. The projection operator can be written in terms of the fermionic operators ψ_k and ψ_k^* . Using the fact that [7]

$$\psi_k^* \psi_k |\lambda\rangle = \begin{cases} 0 & \text{if } k = \lambda_i - i + \frac{1}{2}, \text{ for some } i = 1, 2, 3, \dots \\ |\lambda\rangle & \text{otherwise} \end{cases} \quad (2.44)$$

it is easy to see that the projection operator is given by

$$\mathcal{P}_N = \prod_{j=N+\frac{1}{2}}^{\infty} \psi_j^* \psi_j. \quad (2.45)$$

For the purpose of calculating the generating function it is more useful to write the above projection operator as

$$\mathcal{P}_N = \prod_{j=N+\frac{1}{2}}^{\infty} \psi_j^* \psi_j = \sum_{\eta, \eta_1 \leq N} |\eta\rangle \langle \eta|. \quad (2.46)$$

Thus the refined generating function of the 3D partitions in a $L \times M \times \infty$ box with the restriction that the 2D partition on the diagonal slice through the origin is η . Thus if we want to put a ceiling of height N , we can do this by allowing only those partitions η for which $\eta_1 \leq N$. Thus the generating function of the 3D partitions in a $L \times M \times N$ box is

$$Z(N, M, L) = \sum_{\eta, \eta_1 \leq N} \langle 0 | \prod_{L > m > 0} \Gamma_-(x_m^+) |\eta\rangle \langle \eta | \prod_{0 > m > -M} \Gamma_+(x_m^-) | 0 \rangle. \quad (2.47)$$

Using the expression of the matrix elements in the above in terms of Schur functions

$$\langle \eta | \prod_i \Gamma_+(x_i) | 0 \rangle = \langle 0 | \prod_i \Gamma_-(x_i) |\eta\rangle = s_\eta(\mathbf{x})$$

we get

$$Z(N, M, L) = \sum_{\eta, \eta_1 \leq N} s_\eta(\mathbf{x}^+) s_\eta(\mathbf{x}^-). \quad (2.48)$$

It is easy to see that the above expression satisfies the limiting behavior of $Z(N)$:

$$Z(0, M, L) = 1, \quad Z(\infty, M, L) = \prod_{L > m > 0, 0 > m' > -M} (1 - x_m^+ x_{m'}^-)^{-1}. \quad (2.49)$$

Specializing to the (q, t) parameters by using the previously established map:

$$\begin{aligned} \{x_m^+ | L > m > 0\} &= \{t, t^2, t^3, \dots, t^L\} \\ \{x_m^- | 0 > m > -M\} &= \{1, q, q^2, \dots, q^{M-1}\} \end{aligned}$$

we get

$$Z(N, M, L) = \sum_{\eta, \eta_1 \leq N} s_\eta(t, t^2, t^3, \dots, t^L) s_\eta(1, q, q^2, \dots, q^{M-1}). \quad (2.50)$$

Using the identity

$$s_\eta(1, q, q^2, \dots, q^{M-1}) = q^{n(\eta)} \prod_{s \in \eta} \frac{1 - q^{M+j-i}}{1 - q^{h(s)}}, \quad (2.51)$$

where $n(\eta) = \sum_i (i-1)\eta_i$ we get

$$Z(N, M, L) = \sum_{\eta, \eta_1 \leq N} t^{|\eta|} (tq)^{n(\eta)} \prod_{s \in \eta} \frac{(1-t^{L+j-i})(1-q^{M+j-i})}{(1-t^{h(s)})(1-q^{h(s)})}. \quad (2.52)$$

It is easy to see that if either of L, M or N is equal to 0 then the above generating function reduces to 1 as it should. However, it is easy to see that this crystal partition function is *not* related to the refined partition function of the closed topological vertex geometry X_C ² in any simple way. The refined partition function for X_C is given in Appendix A. It is easy to see that if instead of putting a ceiling in the crystal model we calculate the crystal partition function by weighing the diagonal slice with Q (as in the crystal model of X_0) we get the refined partition function of X_C ,

$$\begin{aligned} Z_{crystal} &= \sum_{\eta} (-Q)^{|\eta|} s_{\eta}(t^{\frac{1}{2}}, t^{\frac{3}{2}}, \dots, t^{M-\frac{1}{2}}) s_{\eta}(q^{\frac{1}{2}}, q^{\frac{3}{2}}, \dots, q^{L-\frac{1}{2}}) \\ &= \frac{Z_{vertex}(Q)}{Z_{vertex}(0)}. \end{aligned} \quad (2.53)$$

Where Z_{vertex} is given by Eq(7.3) given in Appendix A.

3 Adjoint Theory and Periodic Schur Process

In this section, we will discuss the refined crystal model for the 5D $U(1)$ theory with an adjoint hypermultiplet. We will also consider its 4D limit. In 4D this theory has properties similar to the $\mathcal{N} = 4$ theory and is expected to be ultraviolet finite with partition function having modular properties. We will see that the combinatorics of the partition function of this theory is closely related to cylindric partitions [3].

3.1 Geometric Engineering of $U(1)$ Theory with Adjoint Hypermultiplet

We will denote by X_H the geometry which gives rise to $\mathcal{N} = 2$ abelian gauge theory with one adjoint hypermultiplet via compactification of type IIA. The gauge theory is obtained by taking a special limit which we will discuss later. M-theory compactification of X_H gives rise to a $\mathcal{N} = 1$ 5D theory. We will consider this 5D theory on $\mathbb{R}^4 \times S^1$ with the radius of S^1 given by β . The partition function we will compute in the next section using topological vertex formalism is the partition function of the compactified 5D gauge theory.

²This geometry is actually the resolution of the singular geometry $\mathbb{C}^3/\mathbb{Z}_2 \times \mathbb{Z}_2$.

The geometry X_H (and its mirror) was studied in detail in [13, 14, 16, 15] and is the total space of a rank two bundle over an elliptic curve. The rank two bundle is the trivial bundle twisted by a line bundle with first Chern class equal to the mass, m , of the adjoint hypermultiplet. For $m = 0$ we have $\mathcal{N} = 4$ gauge theory as the X_H in this case is simply $E \times \mathbb{C}^2$ where E is an elliptic curve.

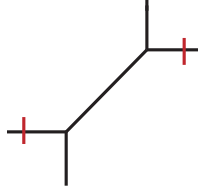


Figure 7: The "toric" diagram of X_H . There are two choices for the preferred direction required by the refined vertex: The internal $(1, 1)$ line or the two vertical external lines.

This geometry X_H can also be obtained by partial compactification of X_0 [15]. In terms of toric diagrams this corresponds to a non-planar toric diagram obtained from the toric diagram of X_0 by gluing two of the parallel external edges. This gives rise to another \mathbb{P}^1 in the geometry such that the new Kähler parameter is proportional to the mass m of the adjoint hypermultiplet. This is shown in Fig. 7. In this case the refined vertex calculation can be done in two different ways corresponding to two different choices for the preferred direction: The

internal $(1, 1)$ line or the two vertical external edges.

3.2 Refined partition function

We begin with the calculation of the refined partition function of this theory using the refined topological vertex formalism [9] and the toric diagram of X_H given above. Recall that the refined vertex calculation requires a preferred direction at each vertex such that all preferred directions of a given toric diagram be parallel³. In the case of X_H we see that there are two choices for the preferred direction corresponding to two seemingly different partition functions. Choosing the

³For an arbitrary toric diagram this may not be possible. An example is the toric diagram of $\mathcal{O}(-3) \mapsto \mathbb{P}^2$. This condition is actually equivalent to requiring that the corresponding CY3-fold be such that it gives rise to a supersymmetric gauge theory via geometric engineering. Thus this CY will be some A_n fibration over a chain of \mathbb{P}^1 's. The preferred direction then corresponds to the base of this fibration.

preferred direction to be the vertical external legs we get:

$$\begin{aligned}
Z^{(1)}(Q, Q_m, t, q) &= \sum_{\lambda, \mu} (-Q_m)^{|\mu|} (-Q)^{|\lambda|} C_{\lambda\mu\emptyset}(t, q) C_{\lambda^t \mu^t \emptyset}(q, t) \\
&= \sum_{\lambda, \mu, \eta_1, \eta_2} (-Q_m)^{|\mu|} (-Q)^{|\lambda|} \left(\frac{q}{t}\right)^{\frac{|\eta_1| - |\eta_2|}{2}} s_{\lambda^t / \eta_1}(t^{-\rho}) s_{\mu / \eta_1}(q^{-\rho}) s_{\lambda / \eta_2}(q^{-\rho}) s_{\mu^t / \eta_2}(t^{-\rho}) \\
&= M(t, q)^{-1} \sum_{\lambda, \mu} Q_{\bullet}^{|\lambda|} s_{\lambda / \mu} \left(t^{-\rho + \frac{1}{2}} q^{-\frac{1}{2}}, Q^{-1} t^{\rho}\right) s_{\lambda / \mu} \left(q^{-\rho}, \sqrt{\frac{q}{t}} Q_m^{-1} q^{\rho}\right) \\
&= \prod_{i, j=1}^{\infty} (1 - Q_m q^{i - \frac{1}{2}} t^{j - \frac{1}{2}}) \widehat{Z}^{(1)}(Q, Q_m, t, q)
\end{aligned} \tag{3.1}$$

where

$$\begin{aligned}
Q &= e^{-T}, \quad Q_m = e^{-T_m}, \quad T, T_m \text{ are the two Kähler parameters} \\
M(t, q) &= \prod_{i, j=1}^{\infty} (1 - t^{i-1} q^j)^{-1}, \quad Q_{\bullet} = Q Q_m \\
\widehat{Z}^{(1)}(Q, Q_m, t, q) &= \sum_{\lambda, \mu} Q^{|\lambda|} Q_m^{|\mu|} s_{\lambda / \mu} \left(-Q_m^{(1)} \sqrt{\frac{q}{t}} q^{\rho}, q^{-\rho}\right) s_{\lambda^t / \mu^t} \left(Q_m^{(2)} \sqrt{\frac{t}{q}} t^{\rho}, t^{-\rho}\right)
\end{aligned} \tag{3.2}$$

On the other hand choosing the internal (1, 1) leg to be the preferred direction we get:

$$\begin{aligned}
Z^{(2)}(Q, Q_m, t, q) &= \sum_{\lambda, \nu} (-Q)^{|\nu|} (-Q_m)^{|\lambda|} C_{\emptyset\lambda\nu}(t, q) C_{\emptyset\lambda^t\nu^t}(q, t) \\
&= \sum_{\nu} (-Q)^{|\nu|} q^{\frac{\|\nu\|^2}{2}} t^{\frac{\|\nu^t\|^2}{2}} \widetilde{Z}_{\nu}(t, q) \widetilde{Z}_{\nu^t}(q, t) \prod_{i, j=1}^{\infty} (1 - Q_m q^{-\mu_i - \rho_j} t^{-\mu_j^t - \rho_i}) \\
&= \prod_{i, j=1}^{+\infty} (1 - Q_m t^{i - \frac{1}{2}} q^{j - \frac{1}{2}}) \widehat{Z}^{(2)}(Q, Q_m, t, q),
\end{aligned} \tag{3.3}$$

where

$$\widehat{Z}^{(2)}(Q, Q_m, t, q) = \sum_{\nu} (Q Q_m)^{|\nu|} \prod_{s \in \nu} \frac{(1 - Q_m t^{a(s) + \frac{1}{2}} q^{\ell(s) + \frac{1}{2}}) (1 - Q_m^{-1} q^{\ell(s) + \frac{1}{2}} t^{a(s) + \frac{1}{2}})}{(1 - t^{a(s) + 1} q^{\ell(s)}) (1 - q^{\ell(s) + 1} t^{a(s)})}. \tag{3.4}$$

Note that:

■ In Eq.(3.2) we have introduced superscripts on $Q_m^{(1)}$ and $Q_m^{(2)}$ just to distinguish the arguments of the skew-Schur function from each other. But we will always take $Q_m^{(1)} = Q_m^{(2)} = Q_m$.

■ In going from Eq. (3.3) to Eq. (3.4) we have used the following identity [?]:

$$\frac{\prod_{i, j=1}^{\infty} (1 - Q_m q^{-\nu_i - \rho_j} t^{-\nu_j^t - \rho_i})}{\prod_{i, j=1}^{\infty} (1 - Q_m q^{-\rho_i} t^{-\rho_j})} = \prod_{s \in \nu} \left(1 - Q_m q^{-\ell(s) - \frac{1}{2}} t^{-a(s) - \frac{1}{2}}\right) \left(1 - Q_m q^{\ell(s) + \frac{1}{2}} t^{a(s) + \frac{1}{2}}\right)$$

The two expressions $Z^{(1)}(Q, Q_m, t, q)$ and $Z^{(2)}(Q, Q_m, t, q)$ (and therefore $\widehat{Z}^{(1)}(Q, Q_m, t, q)$ and $\widehat{Z}^{(2)}(Q, Q_m, t, q)$) appear different but are actually equal to each other as can be seen by expanding them in powers of Q and Q_m therefore from now on we will not use the superscript to distinguish them unless we need a specific form of the partition function. Thus we see that different choices for the preferred direction for a given toric diagram give rise to non-trivial (q, t) identities involving “principal specialization” of the Macdonald function [17]. In section 4 we will give some other examples of (q, t) identities arising from the refined topological vertex calculation.

In the gauge theory language $\widehat{Z}^{(1)}(Q, Q_m, t, q)$ or $\widehat{Z}^{(2)}(Q, Q_m, t, q)$ is the contribution to the gauge theory partition function coming from instantons whereas the prefactor $\prod_{i,j}(1 - Q_m t^{i-\frac{1}{2}} q^{j-\frac{1}{2}})$ is the perturbative contribution. For the moment we will ignore this prefactor and focus only on the instanton contribution. The partition function $Z(Q, Q_m, t, q)$ is invariant under the exchange of Q and Q_m but $\widehat{Z}(Q, Q_m, t, q)$ is not invariant under this exchange.

Using the identity

$$\sum_{\lambda, \mu} Q_{\bullet}^{|\lambda|} s_{\lambda/\mu}(\mathbf{x}) s_{\lambda/\mu}(\mathbf{y}) = \prod_{k=1}^{\infty} \left((1 - Q_{\bullet}^k)^{-1} \prod_{i,j=1}^{\infty} (1 - Q_{\bullet}^k x_i y_j)^{-1} \right), \quad (3.5)$$

we can write $Z(Q, Q_m, t, q)$ in Eq.(3.1) in a product form:

$$\begin{aligned} Z(Q, Q_m, t, q) = M(t, q)^{-1} \prod_{k=1}^{\infty} \left((1 - Q_{\bullet}^k) \prod_{i,j=1}^{\infty} (1 - Q_{\bullet}^k Q_m^{-1} q^{-i+\frac{1}{2}} t^{j-\frac{1}{2}}) (1 - Q_{\bullet}^k Q^{-1} q^{i-\frac{1}{2}} t^{-j+\frac{1}{2}}) \right. \\ \left. \times (1 - Q_{\bullet}^k q^{i-1} t^j) (1 - Q_{\bullet}^{k-1} q^{-i+1} t^{-j}) \right)^{-1}. \end{aligned}$$

If $|t| < 1$ and $|q| < 1$ (i.e., $\epsilon_1 < 0, \epsilon_2 > 0$) then we should write the above as

$$Z(Q, Q_m, t, q) = \prod_{k=1}^{\infty} \left((1 - Q_{\bullet}^k)^{-1} \prod_{i,j=1}^{\infty} \frac{(1 - Q_{\bullet}^k Q_m^{-1} q^{i-\frac{1}{2}} t^{j-\frac{1}{2}}) (1 - Q_{\bullet}^k Q^{-1} q^{i-\frac{1}{2}} t^{j-\frac{1}{2}})}{(1 - Q_{\bullet}^k q^{i-1} t^j) (1 - Q_{\bullet}^k q^i t^{j-1})} \right).$$

On the other hand if $|t| > 1$ and $|q| < 1$ (i.e., $\epsilon_1 > 0, \epsilon_2 > 0$) then we should write the above partition function in terms of q and t^{-1} so that

$$Z(Q, Q_m, t, q) = \prod_{k=1}^{\infty} \left((1 - Q_{\bullet}^k)^{-1} \prod_{i,j} \frac{(1 - Q_{\bullet}^k q^{i-1} t^{1-j}) (1 - Q_{\bullet}^k q^i t^{-j})}{(1 - Q_{\bullet}^k Q_m^{-1} q^{i-\frac{1}{2}} t^{-j+\frac{1}{2}}) (1 - Q_{\bullet}^k Q^{-1} q^{i-\frac{1}{2}} t^{-j+\frac{1}{2}})} \right).$$

3.3 Field theory limit

If we denote the mass of the adjoint by m then the 4D field theory limit is given by⁴

$$Q_m = \sqrt{\frac{t}{q}} e^{-\beta m}, \quad t = e^{\beta \epsilon_1}, \quad q = e^{-\beta \epsilon_2}, \quad \beta \mapsto 0. \quad (3.6)$$

We will see that the two instanton partition functions $\widehat{Z}^{(1)}(Q, Q_m, t, q)$ and $\widehat{Z}^{(2)}(Q, Q_m, t, q)$ give rise to an interesting identity in the above limit. We begin with $\widehat{Z}^{(2)}(Q, Q_m, t, q)$ as it is easy to see what the field theory limit of this is:

$$\begin{aligned} \widehat{Z}^{(2)}(Q, Q_m, t, q) &\xrightarrow{\beta \mapsto 0} \widehat{\mathcal{Z}}(Q, m, \epsilon_1, \epsilon_2) \\ &= \sum_{\nu} Q^{|\nu|} \prod_{s \in \nu} \frac{(a(s) + 1 + \vartheta \ell(s) - \tilde{m})(a(s) + \vartheta(\ell(s) + 1) + \tilde{m})}{(a(s) + 1 + \vartheta \ell(s))(a(s) + \vartheta(\ell(s) + 1))}, \end{aligned}$$

where $\vartheta = -\epsilon_2/\epsilon_1$ and $\tilde{m} = m/\epsilon_1$. The product inside the sum, in the expression above, gives a generalization of Nekrasov-Okounkov probability measure [18] on the set of partitions [19]⁵,

$$\begin{aligned} \prod_{s \in \lambda} \frac{h(s)^2 - \tilde{m}^2}{h(s)^2} &\mapsto \prod_{s \in \lambda} \frac{(a(s) + 1 + \vartheta \ell(s) - \tilde{m})(a(s) + \vartheta \ell(s) + \vartheta + \tilde{m})}{(a(s) + 1 + \vartheta \ell(s))(a(s) + \vartheta \ell(s) + \vartheta)} \\ &\mapsto \prod_{s \in \lambda} \frac{(1 - Q_m t^{a(s)+1} q^{\ell(s)})(1 - Q_m^{-1} q^{\ell(s)+1} t^{a(s)})}{(1 - t^{a(s)+1} q^{\ell(s)})(1 - q^{\ell(s)+1} t^{a(s)})} \end{aligned} \quad (3.7)$$

It was shown in [18] that for $\vartheta = 1$ ($\epsilon_1 + \epsilon_2 = 0$),

$$\widehat{\mathcal{Z}}(Q, m, \epsilon_1, -\epsilon_1) = \prod_{n=1}^{\infty} (1 - Q^n)^{\tilde{m}^2 - 1}. \quad (3.8)$$

Taking the field theory limit of $\widehat{Z}^{(1)}(Q, Q_m, t, q)$ in Eq.(3.2) is slightly more subtle. To take this limit first notice that the argument of the first skew-Schur function in Eq.(3.2) is an infinite set which reduces to a finite set if we take $Q_m^{(1)} = \sqrt{\frac{t}{q}} q^M$ and analytically continue to $|q| < 1$. The same is true for the argument of the second skew-Schur function:

$$\begin{aligned} \{Q_m^{(1)} \sqrt{\frac{q}{t}} q^{\rho}, q^{-\rho}\} &\xrightarrow{Q_m^{(1)} = \sqrt{\frac{t}{q}} q^M} = \{q^{\frac{1}{2}}, q^{\frac{3}{2}}, q^{\frac{5}{2}}, \dots, q^{M-\frac{1}{2}}\} \\ \{Q_m^{(2)} \sqrt{\frac{t}{q}} t^{\rho}, t^{-\rho}\} &\xrightarrow{Q_m^{(2)} = \sqrt{\frac{q}{t}} t^L} = \{t^{\frac{1}{2}}, t^{\frac{3}{2}}, t^{\frac{5}{2}}, \dots, t^{L-\frac{1}{2}}\} \end{aligned} \quad (3.9)$$

⁴In identifying Q_m with the mass m we have introduced a factor of $\sqrt{\frac{t}{q}}$ so that the $m \mapsto 0$ limit gives the partition function of $\mathcal{N} = 4$ gauge theory. For the discussion of the relation between (q, t) and the Ω -background [8] parameters (ϵ_1, ϵ_2) we refer the reader to [9].

⁵ $h(i, j) = a(i, j) + \ell(i, j) + 1$ is the hook length.

With this identification Eq. (3.2) gives

$$\begin{aligned}\widehat{Z}^{(1)}(Q, Q_m, t, q) &= \sum_{\lambda, \mu} (-Q)^{|\lambda|} (-Q_m)^{|\mu|} s_{\lambda/\mu}(q^{\frac{1}{2}}, q^{\frac{3}{2}}, q^{\frac{5}{2}}, \dots, q^{M-\frac{1}{2}}) s_{\lambda^t/\mu^t}(t^{\frac{1}{2}}, t^{\frac{3}{2}}, \dots, t^{L-\frac{1}{2}}) \\ &= \prod_{k=1}^{\infty} \left((1 - Q^k Q_m^k)^{-1} \prod_{i,j=1}^{M,L} (1 - Q^k Q_m^{k-1} q^{i-\frac{1}{2}} t^{j-\frac{1}{2}}) \right).\end{aligned}$$

In the field theory limit given by Eq. (3.6) we get

$$\widehat{Z}^{(1)}(Q, Q_m, t, q) \xrightarrow{\beta \rightarrow 0} \widehat{Z}(Q, m, \epsilon_1, \epsilon_2) = \prod_{k=1}^{\infty} (1 - Q^k)^{ML-1}. \quad (3.10)$$

But since $Q_m^{(1)} = Q_m^{(2)} = \sqrt{\frac{t}{q}} e^{-\beta m}$,

$$\begin{aligned}\sqrt{\frac{t}{q}} q^M &= \sqrt{\frac{q}{t}} t^L \Rightarrow \epsilon_1(L-1) = -\epsilon_2(M-1) \Rightarrow L-1 = \vartheta(M-1), \\ m &= \epsilon_2 M, .\end{aligned} \quad (3.11)$$

which implies that

$$\begin{aligned}ML-1 &= (M-1)(\vartheta M+1) \\ &= -\frac{(m-\epsilon_1)(m-\epsilon_2)}{\epsilon_1 \epsilon_2}.\end{aligned} \quad (3.12)$$

Thus we see that in the field theory limit

$$\widehat{Z}(Q, Q_m, t, q) \xrightarrow{\beta \rightarrow 0} \widehat{Z}(Q, m, \epsilon_1, \epsilon_2) = \prod_{k=1}^{\infty} (1 - Q^k)^{-\frac{(m-\epsilon_1)(m-\epsilon_2)}{\epsilon_1 \epsilon_2}}. \quad (3.13)$$

This gives us the following interesting identity:

$$\sum_{\nu} Q^{|\nu|} \prod_{s \in \nu} \frac{(a(s)+1+\vartheta \ell(s)-\tilde{m})(a(s)+\vartheta(\ell(s)+1)+\tilde{m})}{(a(s)+1+\vartheta \ell(s))(a(s)+\vartheta(\ell(s)+1))} = \prod_{k=1}^{\infty} (1 - Q^k)^{\frac{(\tilde{m}-1)(\tilde{m}+\vartheta)}{\vartheta}}$$

4 Periodic Schur Process

Let us denote by \mathbf{P} the set of Young diagrams. A periodic Schur process is a random process defined on \mathbf{P}^{2K} such that it assigns to a set $\{\lambda^{(a)}, \mu^{(a+1)} \mid a = 0, 1, \dots, K-1\}$ of $2K$ partitions the weight [3]

$$\frac{1}{G_K} \times \varphi^{|\lambda^{(0)}|} \prod_{a=0}^{K-1} s_{\lambda^{(a)}/\mu^{(a+1)}}(\mathbf{x}_{a+1}) s_{\lambda^{(a+1)}/\mu^{(a+1)}}(\mathbf{y}_{a+1}) \quad (4.1)$$

where $\lambda^{(K)} = \lambda^{(0)}$, $\mathbf{x}_a, \mathbf{y}_a$ are specializations of the algebra of symmetric functions and G_K is the partition function of the process,

$$G_K(\varphi, \mathbf{x}, \mathbf{y}) := \sum_{\lambda^{(0)}, \mu^{(1)}, \dots, \lambda^{(K-1)}, \mu^{(K)}} \varphi^{|\lambda^{(0)}|} \prod_{a=0}^{K-1} s_{\lambda^{(a)}/\mu^{(a+1)}}(\mathbf{x}_{a+1}) s_{\lambda^{(a+1)}/\mu^{(a+1)}}(\mathbf{y}_{a+1}). \quad (4.2)$$

We will consider the case when $K = 1$ which is closely related, as we will see, to the counting of cylindric plane partitions. For $K = 1$ the weight assigned to the pair $\{\lambda, \mu\}$ is

$$\frac{1}{G_1} \times s_{\lambda/\mu}(\mathbf{x}) s_{\lambda/\mu}(\mathbf{y}) \quad (4.3)$$

and

$$G_1(\varphi, \mathbf{x}, \mathbf{y}) = \sum_{\lambda, \mu} \varphi^{|\lambda|} s_{\lambda/\mu}(\mathbf{x}) s_{\lambda/\mu}(\mathbf{y}). \quad (4.4)$$

If we take a particular specialization

$$\mathbf{x} = \mathbf{x}(t, q, Q) = \{t^{-\rho+\frac{1}{2}} q^{-\frac{1}{2}}, Q^{-1} t^\rho\} \quad (4.5)$$

$$\mathbf{y} = \mathbf{y}(t, q, Q_m) = \{q^{-\rho}, \sqrt{\frac{q}{t}} Q_m^{-1} q^\rho\}, \quad (4.6)$$

and take $\varphi = Q_\bullet$ then from Eq(3.1) it follows that

$$G_1(Q_\bullet, \mathbf{x}(t, q, Q), \mathbf{y}(t, q, Q_m)) = M(t, q) Z^{(1)}(Q, Q_m, t, q) \quad (4.7)$$

Thus the partition function of the $K = 1$ periodic Schur process is precisely the partition function of the abelian gauge theory with an adjoint hypermultiplet. It was shown in [3] that the $K = 1$ Schur process is related to the counting of cylindric partitions. The cylindric partitions, first introduced in [20], are generalizations of the plane partitions. However, for our purposes, the reparameterization of them in [3] is more suitable, which we largely follow.

A cylindric plane partition of type (n, ℓ) is an infinite array $\{\pi_{i,j} \mid i, j \in \mathbb{Z}\}$ of non-negative numbers such that:

$$\pi_{i,j} \text{ is weakly decreasing in both } i \text{ and } j,$$

$$\pi_{i,j} = \pi_{i+n, j-\ell}.$$

The figure below shows an example of a cylindric partition. It is an infinite periodic diagram with one period shown between the vertical lines. Since the partitions on the vertical lines are identical we can glue them together and instead consider a finite diagram on a cylinder with period $n + \ell$.

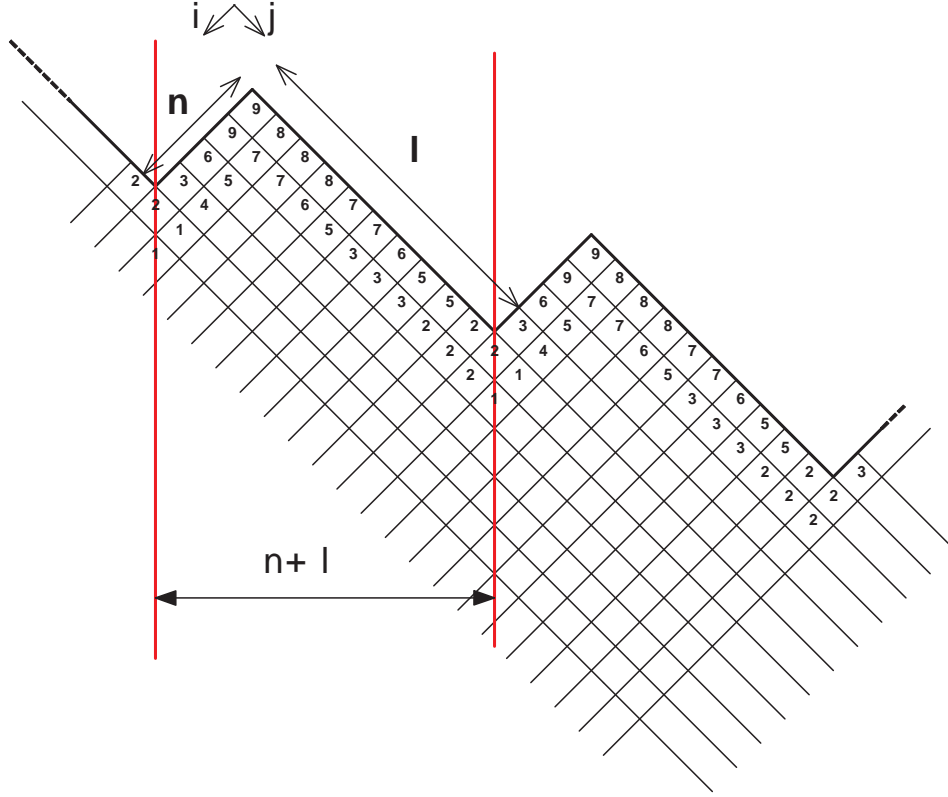


Figure 8: An example for a cylindric partition with $(n, \ell) = (4, 10)$.

Let us define $\mathbb{G}^{n,\ell}(s)$ to be the generating function of cylindric plane partitions of type (n, ℓ) ,

$$\mathbb{G}^{n,\ell}(s) = \sum_{\text{cylindric partitions } \pi \text{ of type } (n, \ell)} s^{|\pi|}, \quad (4.8)$$

where $|\pi| = \sum_{i=1, j=1}^{n, \ell} \pi_{i,j}$. This generating function was determined in [3] and is given by

$$\mathbb{G}^{n,\ell}(s) = \prod_{k=1}^{\infty} \left((1 - s^{k(n+\ell)})^{-1} \prod_{i=1, j=1}^{\ell, n} (1 - s^{k(n+\ell)-i-j+1})^{-1} \right). \quad (4.9)$$

We will show that this generating function is *exactly* the partition function of X_H after an identification of parameters. To see this recall that the partition function of X_H (Eq(3.1)) is given by

$$\begin{aligned} Z^{(1)}(Q, Q_m, t, q) &= M(t, q)^{-1} \mathbb{Z}(Q, Q_m, t, q) \\ \mathbb{Z}(Q, Q_m, t, q) &= \sum_{\lambda, \mu} Q^{|\lambda|} s_{\lambda/\mu} \left(t^{-\rho} \sqrt{\frac{t}{q}}, Q^{-1} t^{\rho} \right) s_{\lambda/\mu} \left(q^{-\rho}, \sqrt{\frac{q}{t}} Q_m^{-1} q^{\rho} \right) \end{aligned} \quad (4.10)$$

The arguments of the two skew-Schur functions in the above equation are an infinite set of variables. By quantizing the two Kähler parameters (and analytic continuation to $|q| < 1, |t| < 1$) we can convert these infinite set of variables into a finite set:

$$\begin{aligned} \{t^i q^{-\frac{1}{2}}, Q^{-1} t^{-i+\frac{1}{2}} \mid i \geq 1\} &\xrightarrow{Q=\sqrt{\frac{q}{t}} t^{-\ell}} \{t^i q^{-\frac{1}{2}} \mid i = 1, 2, \dots, \ell\} \\ \{q^{i-\frac{1}{2}}, \sqrt{\frac{q}{t}} Q_m^{-1} q^{-i+\frac{1}{2}} \mid i \geq 1\} &\xrightarrow{Q_m=\sqrt{\frac{t}{q}} q^{-n}} \{q^{i-\frac{1}{2}} \mid i = 1, 2, \dots, n\} \end{aligned} \quad (4.11)$$

Eq(4.10) becomes

$$\begin{aligned} \mathbb{Z}\left(Q = \sqrt{\frac{q}{t}} t^{-\ell}, Q_m = \sqrt{\frac{t}{q}} q^{-n}, t, q\right) &= \sum_{\lambda, \mu} (t^{-\ell} q^{-n})^{|\lambda|} s_{\lambda/\mu}\left(t q^{-\frac{1}{2}}, t^2 q^{-\frac{1}{2}}, \dots, t^\ell q^{-\frac{1}{2}}\right) \\ &\times s_{\lambda/\mu}\left(q^{\frac{1}{2}}, q^{\frac{3}{2}}, \dots, q^{n-\frac{1}{2}}\right) \\ &= \prod_{k=1}^{\infty} \left((1 - (t^{-\ell} q^{-n})^k) \prod_{i,j=1}^{n,\ell} (1 - q^{i-1-kn} t^{j-k\ell}) \right) \end{aligned}$$

Comparing the above with Eq(4.9) we get

$$\boxed{\mathbb{Z}\left(Q = s^\ell, Q_m = s^n, s^{-1}, s^{-1}\right) = \mathbb{G}^{n,\ell}(s)} \quad (4.12)$$

The two Kähler parameters T, T_m are quantized and given by the positive integers (n, ℓ) which define the type of the cylindric partitions:

$$\begin{aligned} T &= \epsilon_1 \ell + \frac{\epsilon_1 + \epsilon_2}{2} \\ T_m &= -\epsilon_2 n - \frac{\epsilon_1 + \epsilon_2}{2} \end{aligned}$$

5 Hilbert schemes and Vertex Operators

The Hilbert schemes of \mathbb{C}^2 ($\text{Hilb}^\bullet[\mathbb{C}^2]$) play a central role in the Nekrasov's derivation of the gauge theory partition functions using localization [8]. In this section we see that the topological string partition function of X_H can be written in terms of certain vertex operators which are generalization of operators related with the cohomology of the Hilbert scheme $\text{Hilb}^\bullet[\mathbb{C}^2]$ and were studied recently in [5].

Recall that the instanton part of the gauge theory partition function of is given by Eq(3.2),

$$\begin{aligned}\widehat{Z}^{(1)}(Q, Q_m, t, q) &= \sum_{\lambda, \mu} Q^{|\lambda|} Q_m^{|\mu|} s_{\lambda/\mu} \left(-Q_m \sqrt{\frac{q}{t}} q^\rho, q^{-\rho} \right) s_{\lambda^t/\mu^t} \left(Q_m \sqrt{\frac{t}{q}} t^\rho, t^{-\rho} \right) \\ &= \sum_{\lambda, \mu} Q_\bullet^\lambda s_{\lambda/\mu} \left(Q_m \sqrt{\frac{q}{t}} q^\rho, q^{-\rho} \right) s_{\lambda/\mu} \left(Q_m^{-1} t^\rho, \sqrt{\frac{t}{q}} t^{-\rho} \right)\end{aligned}\quad (5.1)$$

Where $Q_\bullet = Q Q_m$ and in going from the first line in the above equation to the second line we have used the properties of the principal specialization of the Schur functions:

$$s_{\lambda^t/\mu^t}(z q^{-\rho}, q^\rho) = (-z)^{|\lambda|-|\mu|} s_{\lambda/\mu}(z^{-1} q^{-\rho}, q^\rho) \quad (5.2)$$

The skew-Schur function in Eq(5.1) can be written as a matrix element of an operator. To see this note that

$$s_{\lambda/\mu}(\mathbf{x}) = \sum_{\eta} c_{\eta\mu}^\lambda s_\eta(\mathbf{x}), \quad (5.3)$$

where $c_{\eta\mu}^\lambda$ are the Littlewood-Richardson coefficients. Let us define an operator $\tilde{\alpha}_\nu$ labeled by a partition ν such that

$$\tilde{\alpha}_\nu |\eta\rangle = \sum_{\lambda} c_{\nu\eta}^\lambda |\lambda\rangle, \quad (5.4)$$

It follows from the above that

$$c_{\nu\eta}^\lambda = \langle \lambda | \tilde{\alpha}_\nu | \eta \rangle = \langle \eta | \tilde{\alpha}_\nu^\dagger | \lambda \rangle. \quad (5.5)$$

Then we see that the skew-Schur function can be written as

$$\begin{aligned}s_{\lambda/\mu}(\mathbf{x}) &= \sum_{\eta} c_{\eta\mu}^\lambda s_\eta(\mathbf{x}) = \sum_{\eta} \langle \lambda | \tilde{\alpha}_\eta | \mu \rangle s_\eta(\mathbf{x}) \\ &= \langle \lambda | \left(\sum_{\eta} s_\eta(\mathbf{x}) \tilde{\alpha}_\eta \right) | \mu \rangle = \langle \mu | \left(\sum_{\eta} s_\eta(\mathbf{x}) \tilde{\alpha}_\eta^\dagger \right) | \lambda \rangle.\end{aligned}\quad (5.6)$$

The operators $\tilde{\alpha}_\nu$ are give by

$$\tilde{\alpha}_\nu = \sum_{\mu} z_\mu^{-1} \chi^\nu(\mu) \alpha_\mu, \quad (5.7)$$

where $z_\mu = 1^{m_1} m_1! 2^{m_2} m_2! \cdots$ for a partition $\mu = (1^{m_1} 2^{m_2} \cdots)$ and χ^μ is the character of the symmetric group. The operator $\alpha_\nu = \alpha_{\nu_1} \alpha_{\nu_2} \cdots$ and $[\alpha_n, \alpha_m] = n \delta_{n+m, 0}$. It is easy to see that in

terms of power sum symmetric functions $p_n(\mathbf{x}) = \sum_i x_i^n$ ⁶

(5.8)

$$\begin{aligned}\mathbb{W}(\mathbf{x}) &= \sum_{\eta} s_{\eta}(\mathbf{x}) \tilde{\alpha}_{\eta} = \sum_{\mu} z_{\mu}^{-1} p_{\mu}(\mathbf{x}) \alpha_{\mu} \\ &= \exp\left(\sum_{n=1}^{\infty} \frac{p_n(\mathbf{x})}{n} \alpha_n\right)\end{aligned}$$

(5.9)

Using the above realization of the skew-Schur function as a matrix element we can write

$$\begin{aligned}\sum_{\lambda, \mu} Q_1^{|\lambda|} Q_2^{|\mu|} s_{\lambda/\mu}(\mathbf{x}) s_{\lambda/\mu}(\mathbf{y}) &= \sum_{\lambda, \mu} Q_1^{|\lambda|} Q_2^{|\mu|} \langle \lambda | \left(\sum_{\eta} s_{\eta}(\mathbf{x}) \tilde{\alpha}_{\eta} \right) | \mu \rangle \langle \mu | \left(\sum_{\eta} s_{\eta}(\mathbf{y}) \tilde{\alpha}_{\eta}^{\dagger} \right) | \lambda \rangle \\ &= \text{Tr}\left(Q_1^H \mathbb{W}(\mathbf{x}) Q_2^H \mathbb{W}(\mathbf{y})^{\dagger}\right)\end{aligned}$$

(5.10)

Where $H|\lambda\rangle = |\lambda| |\lambda\rangle$. Thus the instanton part of the gauge theory partition function can be written as the following trace:

$$\widehat{Z}^{(1)}(Q, Q_m, t, q) = \text{Tr}\left(Q^{\bullet} \exp\left(\sum_{n \geq 1} \frac{q^{\frac{n}{2}}(1-z_1^n)}{n(1-q^n)} \alpha_n\right) \exp\left(\sum_{n \geq 1} \frac{t^n(1-z_2^n)}{n q^{\frac{n}{2}}(1-t^n)} \alpha_{-n}\right)\right),$$

where $z_1 = Q_m \sqrt{\frac{q}{t}}$ and $z_2 = Q_m^{-1} \sqrt{\frac{q}{t}}$. In the 4D field theory limit given by Eq(3.6) the above trace becomes:

$$\widehat{Z}(Q, m, \epsilon_1, \epsilon_2) = \text{Tr}\left(Q^H \exp\left(\frac{m}{\epsilon_2} \sum_{n>0} \frac{1}{n} \alpha_n\right) \exp\left(\frac{m - \epsilon_1 - \epsilon_2}{\epsilon_1} \sum_{n>0} \frac{1}{n} \alpha_{-n}\right)\right)$$

(5.11)

And specializing the Omega background $\epsilon_1 = -\epsilon_2 = 0$ we get ($\tilde{m} = \frac{m}{\epsilon_1} = -\frac{m}{\epsilon_2}$)

$$\begin{aligned}\widehat{Z}(Q, m, -\epsilon_2, \epsilon_2) &= \text{Tr}\left(Q^H \exp\left(-\tilde{m} \sum_{n>0} \frac{1}{n} \alpha_n\right) \exp\left(\tilde{m} \sum_{n>0} \frac{1}{n} \alpha_{-n}\right)\right) \\ &= \sum_{\lambda} Q^{|\lambda|} \langle \lambda | W_{\tilde{m}} | \lambda \rangle\end{aligned}$$

(5.12)

where

$$W_{\tilde{m}} = \exp\left(-\tilde{m} \sum_{n>0} \frac{1}{n} \alpha_n\right) \exp\left(\tilde{m} \sum_{n>0} \frac{1}{n} \alpha_{-n}\right)$$

(5.13)

In [5] it was shown that the vertex operator $W_{\tilde{m}}$ has matrix elements given by intersection over the Hilbert Scheme of \mathbb{C}^2 ,

$$\langle \mu | W_{\tilde{m}} | \lambda \rangle = \int_{\text{Hilb}^k[\mathbb{C}^2] \times \text{Hilb}^l[\mathbb{C}^2]} \omega_{\lambda} \omega_{\mu} e(E),$$

(5.14)

⁶ $p_{\mu}(\mathbf{x}) = p_{\mu_1}(\mathbf{x}) p_{\mu_2}(\mathbf{x}) \cdots = \sum_{\lambda} \chi^{\lambda}(\mu) s_{\lambda}(\mathbf{x}), s_{\lambda}(\mathbf{x}) = \sum_{\mu} z_{\mu}^{-1} \chi^{\lambda}(\mu) p_{\mu}(\mathbf{x}), \sum_{\lambda} \chi^{\lambda}(\mu) \chi^{\lambda}(\nu) = \delta_{\mu, \nu}, \sum_{\mu} z_{\mu}^{-1} \chi^{\lambda}(\mu) \chi^{\nu}(\mu) = \delta_{\lambda, \nu}$.

where ω_λ and ω_μ are the pull-backs to the product of the cohomology classes of $\text{Hilb}^k[\mathbb{C}^2]$ and $\text{Hilb}^l[\mathbb{C}^2]$ respectively. k and l are given by $|\lambda|$ and $|\mu|$ and E is a bundle on the product whose fiber at $(I, J) \in \text{Hilb}^k[\mathbb{C}^2] \times \text{Hilb}^l[\mathbb{C}^2]$ is given by [5]

$$E|_{(I,J)} = \chi(\mathcal{O}(m)) - \chi(I, J \otimes \mathcal{O}(m)). \quad (5.15)$$

The proof of Eq(5.14) was shown to be equivalent to the following identity [5]

$$\langle E^{-\frac{\tilde{m}}{\vartheta}} (E^\dagger)^{\tilde{m}+\theta-1} J_\lambda, J_\mu \rangle_{\vartheta} = (-1)^{|\lambda|+|\mu|} \delta_{\lambda,\mu} \prod_{s \in \lambda} (a(s) + \vartheta(\ell(s) + 1) + \tilde{m}) \prod_{s \in \mu} (a(s) + 1 + \ell(s) \vartheta - \tilde{m}).$$

Where J_λ are the integral form of the Jack polynomials, $E = \exp\left(\sum_{n>0} \frac{(-1)^n}{n} p_n\right)$ and $\langle \cdot, \cdot \rangle_{\vartheta}$ is the ϑ dependent product defined over the ring of symmetric functions. Using the above identity we can write the 4D gauge theory partition function as

$$\begin{aligned} \sum_{\lambda} \varphi^{|\lambda|} \frac{\langle E^{-\frac{\tilde{m}}{\vartheta}} (E^\dagger)^{\tilde{m}+\theta-1} J_\lambda, J_\lambda \rangle_{\vartheta}}{\langle J_\lambda, J_\lambda \rangle_{\vartheta}} &= \sum_{\lambda} (-\varphi)^{|\lambda|} \prod_{s \in \lambda} \frac{(a(s) + \vartheta(\ell(s) + 1) + \tilde{m})(a(s) + 1 + \ell(s) \vartheta - \tilde{m})}{(a(s) + \vartheta(\ell(s) + 1))(a(s) + 1 + \ell(s) \vartheta)} \\ &= \prod_{k=1}^{\infty} (1 - \varphi^k)^{\tilde{m}^2-1}. \end{aligned}$$

Since the two parameter generalization of the Jack polynomials are Macdonald polynomials therefore it is not surprising that the 5D gauge theory partition function can be written using the (q, t) -dependent product $\langle \cdot, \cdot \rangle_{q,t}$ defined on the ring of symmetric functions. This product is defined such that [17]

$$\langle P_\lambda, P_\mu \rangle_{q,t} = \delta_{\lambda,\mu} (-1)^{|\lambda|+|\mu|} \prod_{s \in \lambda} \frac{1 - q^{\ell(s)+1} t^{a(s)}}{1 - q^{\ell(s)} t^{a(s)+1}}. \quad (5.16)$$

The integral form of the Macdonald polynomials $\mathcal{J}_\lambda(t, q)$ is defined as [21]

$$\mathcal{J}_\lambda = \left(\prod_{s \in \lambda} (1 - q^{\ell(s)} t^{a(s)+1}) \right) P_\lambda, \quad (5.17)$$

such that

$$\langle \mathcal{J}_\lambda, \mathcal{J}_\mu \rangle_{q,t} = \delta_{\lambda,\mu} (-1)^{|\lambda|+|\mu|} \prod_{s \in \lambda} (1 - q^{\ell(s)+1} t^{a(s)}) (1 - q^{\ell(s)} t^{a(s)+1}) \quad (5.18)$$

$$\lim_{t \rightarrow 1} \frac{\mathcal{J}|_{q=t^\theta}}{(\text{Int})^{|\lambda|}} = J_\lambda.$$

In terms of this product we can write the 5D gauge theory partition function as

$$\sum_{\lambda} \varphi^{|\lambda|} \frac{\langle \mathcal{G}(Q_m, t, q) \mathcal{J}_\lambda, \mathcal{J}_\lambda \rangle_{q,t}}{\langle \mathcal{J}_\lambda, \mathcal{J}_\lambda \rangle_{q,t}} = \sum_{\nu} \varphi^{|\nu|} \prod_{s \in \nu} \frac{(1 - Q_m t^{a(s)+\frac{1}{2}} q^{\ell(s)+\frac{1}{2}})(1 - Q_m^{-1} q^{\ell(s)+\frac{1}{2}} t^{a(s)+\frac{1}{2}})}{(1 - t^{a(s)+1} q^{\ell(s)})(1 - q^{\ell(s)+1} t^{a(s)})}.$$

Where

$$\begin{aligned}
\mathcal{G}(Q_m, t, q) &= E\left(z_1, 1; q\right) E\left(\sqrt{\frac{t}{q}}z_2, \sqrt{\frac{t}{q}}; t\right)^\dagger \\
E(x, y; q) &= \exp\left(\sum_{n \geq 1} \frac{(-1)^n}{n} \left(\frac{x^n - y^n}{q^{\frac{n}{2}} - q^{-\frac{n}{2}}}\right) p_n\right) \\
z_1 &= Q_m \sqrt{\frac{q}{t}}, \quad z_2 = Q_m^{-1} \sqrt{\frac{q}{t}}.
\end{aligned} \tag{5.19}$$

The adjoint of the operator E is defined with respect to the inner product Eq(5.16). With respect to this inner product if we take p_k to be the operator which multiplies the function with p_k then p_k^\dagger is given by

$$p_k^\dagger = k \left(\frac{1 - t^k}{1 - q^k} \right) \frac{\partial}{\partial p_k}. \tag{5.20}$$

Using the fact that integral form of the Macdonald polynomials can be interpreted as equivariant K-homology classes on $\text{Hilb}^\bullet[\mathbb{C}^2]$ it is possible to realize these operators in terms of equivariant bundles over $\text{Hilb}^\bullet[\mathbb{C}^2]$ [22]. The relation with cylindric partitions suggests that the integral in Eq(5.14) counts the number of cylindric partitions of a certain shape.

6 Refined Topological Vertex and (q, t) Identities

In this section, we will use the refined topological vertex formalism to obtain certain (q, t) identities. Recall that in calculating the partition function of a toric Calabi-Yau threefold using the refined vertex a preferred edge has to be chosen for each vertex such that in the toric diagram all the preferred edges are parallel [9]. For a given toric diagram there may be more than one such choice of the preferred direction. In such a case the expression for the partition function may look different for different choices of the preferred direction giving rise to identities involving the Kähler parameters of the Calabi-Yau threefold and the equivariant parameters q and t .

These identities can also be directly obtained using fiber-base duality of $\mathcal{N} = 2$ gauge theories [6] and Nekrasov's instanton calculus. Given that the refined topological vertex computation can only be done for geometries giving rise to gauge theories (via geometric engineering), the slicing independence of the refined vertex and the fiber-base duality are one and the same thing. We do not provide a rigorous mathematical proof of these identities. In each case we make use of a computer code; we expand each partition function corresponding to a slicing at a certain order in the Kähler parameters and compare term by term. The simplest such identity is the famous summation identity

which relates a sum over Schur functions to a sum over Macdonald functions,

$$\sum_{\nu} \varphi^{\ell(\nu)} s_{\nu}(q^{-\rho}) s_{\nu t}(t^{-\rho}) = \prod_{i,j=1}^{\infty} (1 - \varphi q^{i-\frac{1}{2}} t^{j-\frac{1}{2}}) = \sum_{\nu} \varphi^{\ell(\nu)} P_{\nu}(q^{-\rho}; t, q) P_{\nu t}(t^{-\rho}; q, t).$$

The toric diagram which gives rise to this identity is shown in Fig. 9.



Figure 9: Two choices of the preferred direction labelled by the blue lines.

6.1 Identities

Here we want to demonstrate five explicit examples of identities using the slicing independence of the refined topological vertex.

For *almost* all toric geometries we generically have three distinct choices for the preferred direction. For every internal edge along the preferred direction there is a sum over all partitions and for every internal edge not along the preferred direction the sum can be performed explicitly to give infinite products. However, for each of the three choices of the preferred direction we do not always get a distinct expression. It is possible that two different choices lead indeed to the same expressions with Kähler classes and the corresponding labels for the partitions are appropriately exchanged. We demonstrate examples for this case in the following section.

6.1.1 EXAMPLE 1: $X_0 := \mathcal{O}(-1) \oplus \mathcal{O}(-1) \mapsto \mathbb{P}^1$

Our first example is the toric geometry X_0 . We can use the refined topological vertex to determine the refined partition function. The toric diagram and the two possible choices for the preferred direction are shown in gluing of the refined vertex are shown in Fig. 9. The refined partition function for the choice of the preferred direction shown in Fig. 9(b) is given by

$$\begin{aligned} Z(t, q, Q) &:= \sum_{\nu} (-Q)^{|\nu|} C_{\emptyset \emptyset \nu}(t, q) C_{\emptyset \emptyset \nu t}(q, t) \\ &= \sum_{\nu} \frac{Q^{|\nu|} (-1)^{|\nu|} q^{\frac{\|\nu\|^2}{2}} t^{\frac{\|\nu t\|^2}{2}}}{\prod_{s \in \nu} (1 - t^{a(s)+1} q^{\ell(s)}) (1 - t^{a(s)} q^{\ell(s)+1})}. \end{aligned} \tag{6.1}$$

A different representation of the partition function can be obtained by choosing the preferred directions as shown in Fig. 9(a). The refined partition function with this choice is given by

$$\begin{aligned} Z(t, q, Q) &= \sum_{\lambda} (-Q)^{|\lambda|} C_{\lambda \emptyset \emptyset}(t, q) C_{\lambda^t \emptyset \emptyset}(q, t) = \sum_{\lambda} (-Q)^{|\lambda|} s_{\lambda^t}(t^{-\rho}) s_{\lambda^t}(q^{-\rho}) \\ &= \prod_{i,j=1}^{\infty} (1 - Q q^{i-\frac{1}{2}} t^{j-\frac{1}{2}}) = \text{Exp} \left\{ - \sum_{n=1}^{\infty} \frac{Q^n}{n(q^{\frac{n}{2}} - q^{-\frac{n}{2}})(t^{\frac{n}{2}} - t^{-\frac{n}{2}})} \right\}. \end{aligned}$$

Identifying the above two representations of the partition function we get the following identity

$$\sum_{\nu} \frac{Q^{|\nu|} (-1)^{|\nu|} q^{\frac{\|\nu\|^2}{2}} t^{\frac{\|\nu^t\|^2}{2}}}{\prod_{s \in \nu} (1 - t^{a(s)+1} q^{\ell(s)}) (1 - t^{a(s)} q^{\ell(s)+1})} = \text{Exp} \left\{ - \sum_{n=1}^{\infty} \frac{Q^n}{n(q^{\frac{n}{2}} - q^{-\frac{n}{2}})(t^{\frac{n}{2}} - t^{-\frac{n}{2}})} \right\} \quad (6.2)$$

which is a specialization of the identity Eq. (5.4) of [17] and was also derived in [?].

6.1.2 EXAMPLE 2: $\mathcal{O}(0) \oplus \mathcal{O}(-2) \mapsto \mathbb{P}^1$

This geometry can be obtained from local $\mathbb{P}^1 \times \mathbb{P}^1$ by taking the size of one of the \mathbb{P}^1 very large and is the resolution of $\mathbb{C} \times \mathbb{C}^2/\mathbb{Z}_2$. The toric geometry and the two possible choices for the preferred direction are shown in the Fig. 10 below.

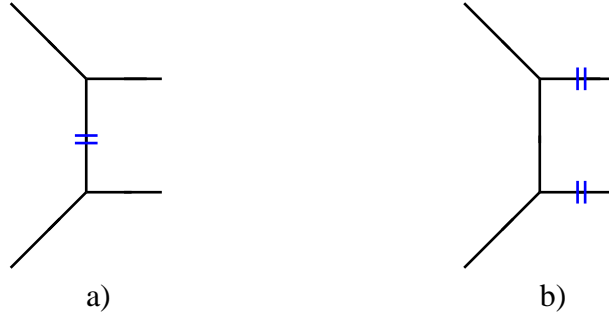


Figure 10: Two possible choices for the preferred direction, the internal line (a) and the parallel external lines (b).

The refined partition function for the case Fig. 10(a) is given by

$$\begin{aligned} Z(t, q, Q) &= \sum_{\nu} Q^{|\nu|} (-1)^{|\nu|} C_{\emptyset \emptyset \nu}(t, q) f_{\nu}(t, q) C_{\emptyset \emptyset \nu^t}(q, t) \quad (6.3) \\ &= \sum_{\nu} (-Q)^{|\nu|} \tilde{Z}_{\nu}(t, q) \tilde{Z}_{\nu^t}(q, t) q^{\frac{\|\nu\|^2}{2}} t^{\frac{\|\nu^t\|^2}{2}} f_{\nu}(t, q) \\ &= \sum_{\nu} \frac{(Q \sqrt{\frac{q}{t}})^{|\nu|} t^{\|\nu^t\|^2}}{\prod_{s \in \nu} (1 - t^{a(s)+1} q^{\ell(s)}) (1 - t^{a(s)} q^{\ell(s)+1})}. \end{aligned}$$

The partition function for case (b) of Fig. 10 is given by,

$$\begin{aligned}
Z(t, q, Q) &= \sum_{\lambda} Q^{|\lambda|} (-1)^{|\lambda|} C_{\emptyset \lambda \emptyset}(t, q) f_{\lambda}(t, q) C_{\lambda \emptyset \emptyset}(t, q) \\
&= \sum_{\lambda} (-Q)^{|\lambda|} \left(\frac{q}{t}\right)^{\frac{\|\lambda\|^2}{2}} t^{-\frac{\kappa(\lambda)}{2}} s_{\lambda^t}(q^{-\rho}) f_{\lambda}(t, q) s_{\lambda}(t^{-\rho}) \\
&= \sum_{\lambda} (Q \sqrt{\frac{q}{t}})^{|\lambda|} s_{\lambda^t}(t^{-\rho}) s_{\lambda^t}(q^{-\rho}) = \prod_{i,j=1}^{\infty} \left(1 - Q q^i t^{j-1}\right)^{-1} \\
&= \text{Exp} \left\{ \sum_{n=1}^{\infty} \frac{Q^n \left(\frac{q}{t}\right)^{\frac{n}{2}}}{n(q^{\frac{n}{2}} - q^{-\frac{n}{2}})(t^{\frac{n}{2}} - t^{-\frac{n}{2}})} \right\}.
\end{aligned} \tag{6.4}$$

Thus we get the identity (after rescaling Q and interchanging q and t)

$$\sum_{\nu} \frac{Q^{|\nu|} q^{\|\nu^t\|^2}}{\prod_{s \in \nu} (1 - q^{a(s)+1} t^{\ell(s)})(1 - q^{a(s)} t^{\ell(s)+1})} = \text{Exp} \left\{ \sum_{n=1}^{\infty} \frac{Q^n \left(\frac{q}{t}\right)^{\frac{n}{2}}}{n(q^{\frac{n}{2}} - q^{-\frac{n}{2}})(t^{\frac{n}{2}} - t^{-\frac{n}{2}})} \right\}. \tag{6.5}$$

6.1.3 EXAMPLE 3

Our third example is that of the geometry giving rise to 5D $U(1)$ gauge theory with a single adjoint. The toric diagram of this geometry is shown in Fig. 11 below. Fig. 11(a) and Fig. 11(b)

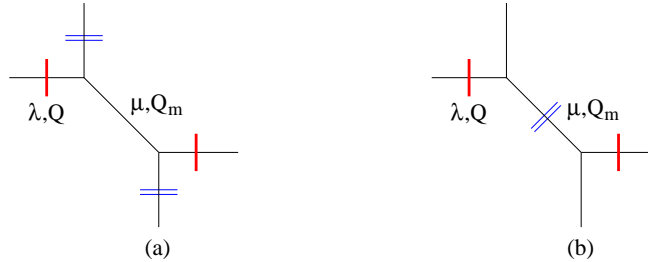


Figure 11: The toric diagram for the geometry giving rise to 5D supersymmetric $U(1)$ theory with adjoint matter.

show two possible choices for the preferred direction needed for refined vertex calculation. The single thick line indicates the gluing of the corresponding edges giving rise to non-planar diagrams.

In Fig. 11(a) the preferred direction is along the non-compact edges whereas in Fig. 11(b) the preferred direction is along one of the compact edge.

The refined vertex calculation for Fig. 11(a) gives:

$$\begin{aligned}
Z_{(a)} &= \sum_{\lambda, \mu} (-Q_m)^{|\mu|} (-Q)^{|\lambda|} C_{\lambda \mu \emptyset}(t, q) C_{\lambda^t \mu^t \emptyset}(q, t) \\
&= \sum_{\lambda, \mu, \eta_1, \eta_2} (-Q_m)^{|\mu|} (-Q)^{|\lambda|} \left(\frac{q}{t}\right)^{\frac{|\eta_1| - |\eta_2|}{2}} s_{\lambda^t / \eta_1}(t^{-\rho}) s_{\mu / \eta_1}(q^{-\rho}) s_{\lambda / \eta_2}(q^{-\rho}) s_{\mu^t / \eta_2}(t^{-\rho}) \\
&= \prod_{i', j'=1}^{\infty} (1 - Q_m q^{-\rho_{i'}} t^{-\rho_{j'}}) \prod_{k=1}^{\infty} \left[(1 - Q^k Q_m^k)^{-1} \prod_{i, j=1}^{\infty} (1 - Q^k Q_m^{k-1} q^{-\rho_i} t^{-\rho_j}) \right. \\
&\quad \left. (1 - Q^k Q_m^k q^{\rho_i - 1/2} t^{-\rho_j + 1/2}) (1 - Q^k Q_m^k q^{-\rho_i + 1/2} t^{\rho_j - 1/2}) (1 - Q^k Q_m^{k+1} q^{\rho_i} t^{\rho_j}) \right].
\end{aligned} \tag{6.6}$$

Changing the preferred direction changes the expression of the refined vertex calculation and therefore Fig. 11(b) gives:

$$\begin{aligned}
Z_{(b)} &= \sum_{\lambda, \mu} (-Q_m)^{|\mu|} (-Q)^{|\lambda|} C_{\emptyset \lambda \mu}(t, q) C_{\emptyset \lambda^t \mu^t}(q, t) \\
&= \sum_{\mu} (-Q_m)^{|\mu|} \left(\frac{q}{t}\right)^{\frac{\|\mu\|^2 - \|\mu^t\|^2}{2}} P_{\mu^t}(t^{-\rho}; q, t) P_{\mu}(q^{-\rho}; t, q) \prod_{i, j=1}^{\infty} (1 - Q q^{-\mu_i - \rho_j} t^{-\mu_j^t - \rho_i})
\end{aligned} \tag{6.7}$$

6.1.4 EXAMPLE 4

The toric diagram of the geometry which gives rise to 5D U(1) gauge theory with two hypermultiplets in the fundamental representation is given in Fig. 12 below.

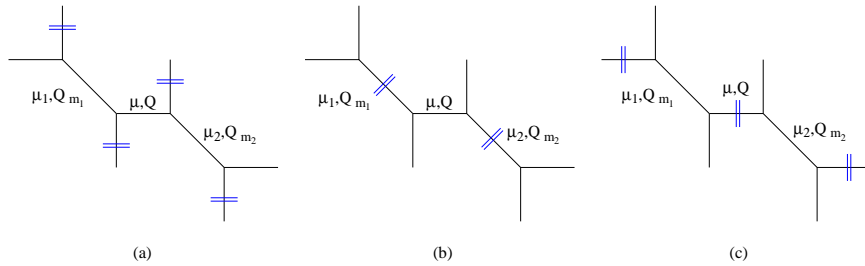


Figure 12: The toric diagram for the 5D supersymmetric $U(1)$ theory with $N_f = 2$. The three distinct choices of the preferred direction lead to three distinct expressions, with a) no sums over partitions, with b) two sums over partitions and with c) one sum over partitions.

The choice of the preferred direction is indicated by the short double line. In this case there are three different choices for the preferred direction giving rise to three seemingly different expressions for the refined partition function.

Fig. 12(a) gives:

$$\begin{aligned}
Z_{(a)} &= \sum_{\mu, \mu_1, \mu_2} (-Q)^{|\mu|} (-Q_{m_1})^{|\mu_1|} (-Q_{m_2})^{|\mu_2|} C_{\emptyset \mu_1 \emptyset}(t, q) C_{\mu \mu_1^t \emptyset}(q, t) C_{\mu^t \mu_2 \emptyset}(t, q) C_{\emptyset \mu_2^t \emptyset}(q, t) \quad (6.8) \\
&= \sum_{\mu, \mu_1, \mu_2, \eta_1, \eta_2} (-Q)^{|\mu|} (-Q_{m_1})^{|\mu_1|} (-Q_{m_2})^{|\mu_2|} \left(\frac{t}{q}\right)^{\frac{|\eta_1| - |\eta_2|}{2}} s_{\mu_1}(q^{-\rho}) s_{\mu_1^t / \eta_1}(t^{-\rho}) s_{\mu^t / \eta_1}(q^{-\rho}) \\
&\times s_{\mu / \eta_2}(t^{-\rho}) s_{\mu_2 / \eta_2}(q^{-\rho}) s_{\mu_2^t}(t^{-\rho}) \\
&= \prod_{i, j=1}^{\infty} \frac{(1 - Q q^{-\rho_i} t^{-\rho_j})(1 - Q_{m_1} q^{-\rho_i} t^{-\rho_j})(1 - Q_{m_2} q^{-\rho_i} t^{-\rho_j})(1 - Q Q_{m_1} Q_{m_2} q^{-\rho_i} t^{-\rho_j})}{(1 - Q Q_{m_1} q^{-\rho_i - 1/2} t^{-\rho_j + 1/2})(1 - Q Q_{m_2} q^{-\rho_i + 1/2} t^{-\rho_j - 1/2})}
\end{aligned}$$

Fig. 12(b) gives:

$$\begin{aligned}
Z_{(b)} &= \sum_{\mu, \mu_1, \mu_2} (-Q)^{|\mu|} (-Q_{m_1})^{|\mu_1|} (-Q_{m_2})^{|\mu_2|} C_{\emptyset \emptyset \mu_1}(t, q) C_{\emptyset \mu \mu_1^t}(q, t) C_{\emptyset \mu^t \mu_2}(t, q) C_{\emptyset \emptyset \mu_2^t}(q, t) \\
&= \sum_{\mu_1, \mu_2} (-Q_{m_1})^{|\mu_1|} (-Q_{m_2})^{|\mu_2|} \left(\frac{q}{t}\right)^{\frac{\|\mu_1\|^2 - \|\mu_1^t\|^2 + \|\mu_2\|^2 - \|\mu_2^t\|^2}{2}} P_{\mu_1^t}(t^{-\rho}; q, t) P_{\mu_1}(q^{-\rho}; t, q) P_{\mu_2^t}(t^{-\rho}; q, t) \\
&\times P_{\mu_2}(q^{-\rho}; t, q) \prod_{i, j=1}^{\infty} (1 - Q q^{-\mu_{1,i} - \rho_j} t^{-\mu_{2,j} - \rho_i})
\end{aligned}$$

Fig. 12(c) gives:

$$\begin{aligned}
Z_{(c)} &= \sum_{\mu, \mu_1, \mu_2} (-Q)^{|\mu|} (-Q_{m_1})^{|\mu_1|} (-Q_{m_2})^{|\mu_2|} C_{\mu_1 \emptyset \emptyset}(t, q) C_{\mu_1^t \emptyset \mu}(q, t) C_{\mu_2 \emptyset \mu^t}(t, q) C_{\mu_2^t \emptyset \emptyset}(q, t) \\
&= \sum_{\mu} (-Q)^{|\mu|} \left(\frac{t}{q}\right)^{\frac{\|\mu\|^2 - \|\mu^t\|^2}{2}} P_{\mu^t}(q^{-\rho}; t, q) P_{\mu}(t^{-\rho}; q, t) \\
&\times \prod_{i, j=1}^{\infty} (1 - Q_{m_1} q^{-\rho_i} t^{-\mu_i - \rho_j})(1 - Q_{m_2} q^{-\mu_i^t - \rho_j} t^{-\rho_i})
\end{aligned}$$

FLOP TRANSITION

In this case there are only two different choices for the preferred direction.

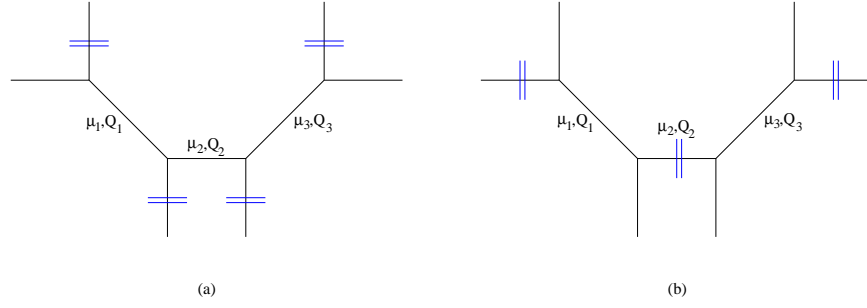


Figure 13: The flop transition relates this geometry with that of Fig. 12. The corresponding geometrically engineered gauge theory has masses of hypermultiplets of different signs.

Fig. 13(a) gives:

$$\begin{aligned}
Z_{(a)} &= \sum_{\mu_1, \mu_2, \mu_3} (-Q_1)^{|\mu_1|} (-Q_2)^{|\mu_2|} (-Q_3)^{|\mu_3|} C_{\mu_3 \emptyset \emptyset}(q, t) C_{\mu_3^\dagger \mu_2 \emptyset}(t, q) f_{\mu_2}(t, q) C_{\mu_2^\dagger \mu_1 \emptyset}(t, q) C_{\emptyset \mu_1^\dagger \emptyset}(q, t) \\
&= \prod_{i, j=1}^{\infty} \frac{(1 - Q_1 q^{-\rho_i} t^{-\rho_j})(1 - Q_3 q^{-\rho_i} t^{-\rho_j})(1 - Q_1 Q_2 q^{-\rho_i+1} t^{-\rho_j-1})(1 - Q_2 Q_3 q^{-\rho_i+1} t^{-\rho_j-1})}{(1 - Q_2 q^{-\rho_i+1/2} t^{-\rho_j-1/2})(1 - Q_1 Q_2 Q_3 q^{-\rho_i+3/2} t^{-\rho_j-3/2})}
\end{aligned}$$

Fig. 13(b) gives:

$$\begin{aligned}
Z_{(b)} &= \sum_{\mu_1, \mu_2, \mu_3} (-Q_1)^{|\mu_1|} (-Q_2)^{|\mu_2|} (-Q_3)^{|\mu_3|} C_{\emptyset \mu_3 \emptyset}(q, t) C_{\emptyset \mu_3^\dagger \mu_2}(t, q) f_{\mu_2}(t, q) C_{\mu_1 \emptyset \mu_2^\dagger}(q, t) C_{\mu_1^\dagger \emptyset \emptyset}(t, q) \\
&= \sum_{\mu_2} (-\tilde{Q}_2 q^{1/2} t^{-1/2})^{|\mu_2|} t^{\|\mu_2^\dagger\|^2} t^{-\|\mu_2\|^2/2} P_{\mu_2^\dagger}(t^{-\rho}; q, t) q^{-\|\mu_2^\dagger\|^2/2} P_{\mu_2}(q^{-\rho}; t, q) \prod_{i, j=1}^{\infty} (1 - Q_1 q^{-\rho_i} t^{-\mu_{2,i}^\dagger - \rho_j}) \\
&\quad \times (1 - Q_3 q^{-\rho_i} t^{-\mu_{2,i}^\dagger - \rho_j})
\end{aligned}$$

6.1.5 EXAMPLE 5

Our final example is of the geometry giving rise to a quiver gauge theory with gauge group $U(1) \times U(1)$. This theory, its generalization with $U(k)^N$ gauge group and the corresponding geometries were studied in [15] to which we refer the reader for more details.

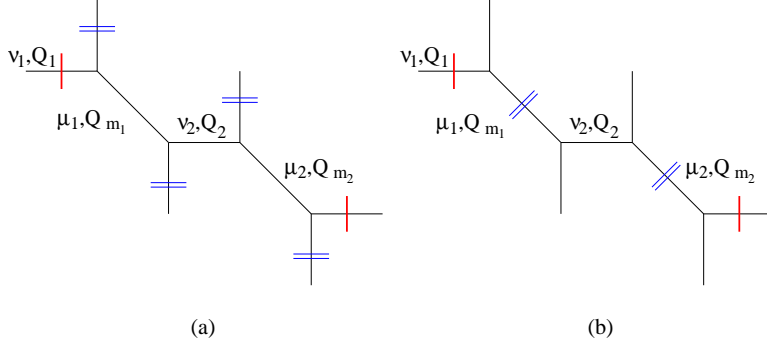


Figure 14: The toric diagram for the 5D \hat{A}_0 quiver theory. The three distinct choices of the preferred directions are not all distinct, the other choice, picking the preferred direction along ν 's will have basically the same form as the one in b).

Fig. 14(a) gives:

$$\begin{aligned}
Z_{(a)} &= \sum_{\mu_1, \mu_2, \nu_1, \nu_2} (-Q_{m_1})^{|\mu_1|} (-Q_{m_2})^{|\mu_2|} (-Q_1)^{|\nu_1|} (-Q_2)^{|\nu_2|} C_{\nu_1 \mu_1 \emptyset}(t, q) C_{\nu_2 \mu_1^t \emptyset}(q, t) C_{\nu_2^t \mu_2 \emptyset}(t, q) C_{\nu_1^t \mu_2^t \emptyset}(q, t) \\
&= \sum_{\substack{\mu_1, \mu_2, \nu_1, \nu_2, \\ \eta_1, \eta_2, \eta_3, \eta_4}} (-Q_{m_1})^{|\mu_1|} (-Q_{m_2})^{|\mu_2|} (-Q_1)^{|\nu_1|} (-Q_2)^{|\nu_2|} \left(\frac{q}{t}\right)^{\frac{|\eta_1| - |\eta_2| + |\eta_3| - |\eta_4|}{2}} s_{\nu_1^t / \eta_1}(t^{-\rho}) s_{\mu_1 / \eta_1}(q^{-\rho}) \\
&\quad s_{\nu_2^t / \eta_2}(q^{-\rho}) s_{\mu_1^t / \eta_2}(t^{-\rho}) s_{\nu_2 / \eta_3}(t^{-\rho}) s_{\mu_2 / \eta_3}(q^{-\rho}) s_{\nu_1 / \eta_4}(q^{-\rho}) s_{\mu_2^t / \eta_4}(t^{-\rho}) \\
&= \prod_{i,j=1}^{\infty} \frac{(1 - Q_1 q^{-\rho_i} t^{-\rho_j})(1 - Q_2 q^{-\rho_i} t^{-\rho_j})(1 - Q_{m_1} Q_2 q^{\rho_i - 1/2} t^{-\rho_j + 1/2})(1 - Q_{m_1} Q_1 Q_2 q^{-\rho_i} t^{-\rho_j})}{(1 - Q_{m_1} q^{\rho_i} t^{-\rho_j})(1 - Q_{m_1} Q_1 q^{-\rho_i + 1/2} t^{-\rho_j - 1/2})} \\
&\quad \times \sum_{\mu_2, \lambda} (-Q_{m_2})^{|\mu_2|} (-Q_{m_1} Q_1 Q_2)^{|\lambda|} s_{\mu_2^t / \lambda}(q^\rho, Q_2 q^{-\rho + 1/2} t^{-1/2}, Q_{m_1} Q_2 q^\rho, Q_{m_1} Q_1 Q_2 q^{-\rho + 1/2} t^{-1/2}) \\
&\quad \times s_{\mu_2 / \lambda}(t^\rho, Q_1 t^{-\rho + 1/2} q^{-1/2}, Q_{m_1} Q_1 t^\rho, Q_{m_1} Q_1 Q_2 t^{-\rho + 1/2} q^{-1/2})
\end{aligned}$$

Fig. 14(b) gives:

$$\begin{aligned}
Z_{(b)} &= \sum_{\mu_1, \mu_2, \nu_1, \nu_2} (-Q_{m_1})^{|\mu_1|} (-Q_{m_2})^{|\mu_2|} (-Q_1)^{|\nu_1|} (-Q_2)^{|\nu_2|} C_{\emptyset \nu_1 \mu_1}(t, q) C_{\emptyset \nu_2 \mu_1^t}(q, t) C_{\emptyset \nu_2^t \mu_2}(t, q) C_{\emptyset \nu_1^t \mu_2^t}(q, t) \\
&= \sum_{\mu_1, \mu_2} (-Q_{m_1})^{|\mu_1|} (-Q_{m_2})^{|\mu_2|} (-Q_1)^{|\nu_1|} (-Q_2)^{|\nu_2|} \left(\frac{q}{t}\right)^{\frac{\|\mu_1\|^2 - \|\mu_1^t\|^2 + \|\mu_2\|^2 - \|\mu_2^t\|^2}{2}} P_{\mu_1^t}(t^{-\rho}; q, t) P_{\mu_1}(q^{-\rho}; t, q) \\
&\quad \times P_{\mu_2^t}(t^{-\rho}; q, t) P_{\mu_2}(q^{-\rho}; t, q) \prod_{i,j}^{\infty} (1 - Q_1 q^{-\mu_2, i - \rho_j} t^{-\mu_{1,j}^t - \rho_i})(1 - Q_2 q^{-\mu_{1,i} - \rho_j} t^{-\mu_{2,j}^t - \rho_i})
\end{aligned}$$

Acknowledgments

AI and CK would like to thank Charles Doran for many valuable discussions.

7 Appendix A

In this section we want to sketch the refined topological vertex computations for the resolved conifold, double- \mathbb{P}^1 and the closed refined topological vertex.

RESOLVED CONIFOLD

Fig. 15 shows the toric diagram of resolved conifold and our choice of $\{t, q\}$ -parametrization. The double blue lines again show the preferred direction of the refined topological vertex. The partition function is given by

$$\begin{aligned} Z_{\text{vertex}} &= \sum_{\mu} (-Q)^{|\mu|} C_{\emptyset\mu\emptyset}(t, q) C_{\emptyset\mu^t\emptyset}(q, t) \quad (7.1) \\ &= \sum_{\mu} (-Q)^{|\mu|} s_{\mu}(q^{-\rho}) s_{\mu^t}(t^{-\rho}) \\ &= \prod_{i=1}^{\infty} \prod_{j=1}^{\infty} (1 - Qt^{i-1/2} q^{j-1/2}) \end{aligned}$$

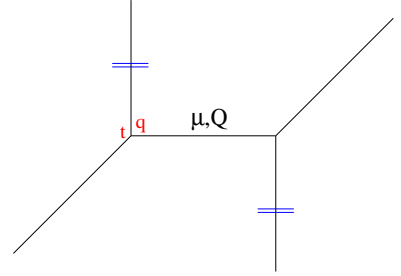


Figure 15: Toric diagram of resolved conifold

DOUBLE- \mathbb{P}^1

Fig. 16 shows the toric diagram of double- \mathbb{P}^1 . The partition function reads

$$\begin{aligned} Z_{\text{vertex}} &= \sum_{\mu_1, \mu_2} (-Q_1)^{|\mu_1|} (-Q_2)^{|\mu_2|} C_{\emptyset\mu_1\emptyset}(q, t) C_{\mu_2\mu_1^t\emptyset}(t, q) C_{\mu_2^t\emptyset\emptyset}(q, t) \\ &= \sum_{\mu_1, \mu_2, \eta} (-Q_1)^{|\mu_1|} (-Q_2)^{|\mu_2|} \left(\frac{q}{t}\right)^{|\eta|/2} s_{\mu_1}(t^{-\rho}) s_{\mu_1^t/\eta}(q^{-\rho}) \quad (7.2) \\ &\quad \times s_{\mu_2}(q^{-\rho}) s_{\mu_2^t/\eta}(t^{-\rho}) \\ &= \prod_{i=1}^{\infty} \prod_{j=1}^{\infty} \frac{(1 - Q_1 t^{i-1/2} q^{j-1/2}) (1 - Q_2 t^{i-1/2} q^{j-1/2})}{(1 - Q_1 Q_2 t^{i-1} q^j)} \end{aligned}$$

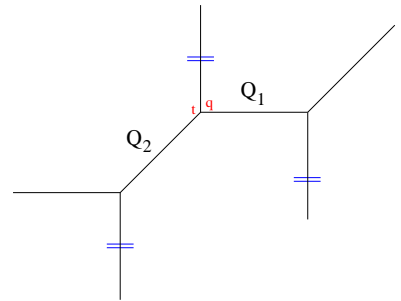


Figure 16: Toric diagram of double- \mathbb{P}^1

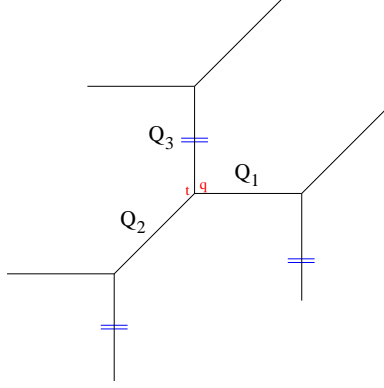


Figure 17: Toric diagram of closed refined topological vertex

CLOSED REFINED TOPOLOGICAL VERTEX

Fig. 17 shows the toric diagram of closed refined topological vertex. The partition function reads

$$\begin{aligned}
Z_{\text{vertex}}(Q_3) &:= \sum_{\mu_1, \mu_2, \mu_3} (-Q_1)^{|\mu_1|} (-Q_2)^{|\mu_2|} (-Q_3)^{|\mu_3|} C_{\emptyset \emptyset \mu_3}(q, t) C_{\mu_2 \mu_1^t \mu_3^t}(t, q) C_{\mu_2^t \emptyset \emptyset}(q, t) C_{\emptyset \mu_1 \emptyset}(q, t) \\
&= \sum_{\mu_1, \mu_2, \mu_3, \eta} (-Q_1)^{|\mu_1|} (-Q_2)^{|\mu_2|} (-Q_3)^{|\mu_3|} \left(\frac{q}{t}\right)^{|\eta|/2} \left(\frac{t}{q}\right)^{\|\mu_3\|^2/2} \\
&\quad \times P_{\mu_3^t}(q^{-\rho}; t, q) \left(\frac{q}{t}\right)^{\|\mu_3^t\|^2/2} P_{\mu_3}(t^{-\rho}; q, t) s_{\mu_1}(t^{-\rho}) s_{\mu_1^t/\eta}(t^{-\mu_3} q^{-\rho}) \\
&\quad \times s_{\mu_2}(q^{-\rho}) s_{\mu_2^t/\eta}(t^{-\rho} q^{-\mu_3^t}) \\
&= \sum_{\mu_3} (-Q_3)^{|\mu_3|} \left(\frac{t}{q}\right)^{\frac{\|\mu_3\|^2 - \|\mu_3^t\|^2}{2}} P_{\mu_3^t}(q^{-\rho}; t, q) P_{\mu_3}(t^{-\rho}; q, t) \\
&\quad \times \prod_{i=1}^{\infty} \prod_{j=1}^{\infty} \frac{(1 - Q_1 t^{-\mu_3, i+j-1/2} q^{j-1/2})(1 - Q_2 q^{-\mu_3^t, i+j-1/2} t^{i-1/2})}{(1 - Q_1 Q_2 t^{i-1} q^j)} \tag{7.3}
\end{aligned}$$

8 Appendix B: Useful Identities

In this section, we want to give a short list of identities [17] or definitions which we have used in our computations. We also include a short proof of generalizing one of the identities.

The Schur functions define a basis for the symmetric function and the skew Schur functions $s_{\lambda/\mu}(x_1, x_2, \dots)$ have the following nice representation as a sum over all semi-standard Young tableau λ/μ :

$$s_{\lambda/\mu}(x_1, x_2, \dots) = \sum_{T_{\lambda/\mu}} x_1^{m_1} x_2^{m_2} \dots \quad (8.1)$$

where m_i is the degeneracy of i in the tableau. The Macdonald function $P_\nu(t^{-\rho}; q, t)$ is defined by

$$P_\nu(t^{-\rho}; q, t) = t^{\|\nu^t\|/2} \tilde{Z}_\nu(t, q), \quad (8.2)$$

where $\rho_i = 1/2 - i$ and

$$\tilde{Z}_\nu(t, q) = \prod_{s \in \nu} \frac{1}{1 - t^{a(s)+1} q^{\ell(s)}}. \quad (8.3)$$

with $a(s) = \nu_j^t - i$ and $\ell(s) = \nu_i - j$ being the arm and leg length of $s = (i, j) \in \nu$, respectively. The Schur functions have the following properties:

$$s_{\lambda/\mu}(x^{(1)}, \dots, x^{(n)}) = \sum_{(\nu)} \prod_{i=1}^n s_{\nu^{(i)}/\nu^{(i-1)}}(x^{(i)}), \quad (8.4)$$

where we have defined $\nu^{(0)} \equiv \mu$ and $\nu^{(n)} \equiv \lambda$. Note that $\nu^{(i-1)} \prec \nu^{(i)}$.

$$s_{\lambda/\mu}(q^{-\rho}) = s_{\lambda^t/\mu^t}(-q^\rho) \quad (8.5)$$

We extensively made use of the following sums

$$\sum_{\eta} s_{\eta/\nu}(x) s_{\eta/\mu}(y) = \prod_{i,j=1}^{\infty} (1 - x_i y_j)^{-1} \sum_{\tau} s_{\mu/\tau}(x) s_{\nu/\tau}(y), \quad (8.6)$$

$$\sum_{\eta} s_{\eta^t/\nu}(x) s_{\eta/\mu}(y) = \prod_{i,j=1}^{\infty} (1 + x_i y_j) \sum_{\tau} s_{\mu^t/\tau}(x) s_{\nu^t/\tau}(y), \quad (8.7)$$

where the right hand side of the equations reduce to the product if μ or ν is equal to the empty partition, since $s_{\emptyset/\tau} = 1$ for $\tau = \emptyset$ and vanishes for any other τ . The following product forms are known for the case of $\mu = \nu$ in the above identities and we also sum the left hand side over μ

$$\sum_{\rho, \lambda} q^{|\rho|} s_{\rho/\lambda}(x) s_{\rho/\lambda}(y) = \prod_{k=1}^{\infty} (1 - q^k)^{-1} \prod_{i,j=1}^{\infty} (1 - q^k x_i y_j)^{-1} \quad (8.8)$$

$$\sum_{\rho, \lambda} q^{|\rho|} s_{\rho^t/\lambda}(x) s_{\rho/\lambda^t}(y) = \prod_{k=1}^{\infty} (1 - q^k)^{-1} \prod_{i,j=1}^{\infty} (1 + q^k x_i y_j). \quad (8.9)$$

These last two identities are the ones we wan to generalize in the following way⁷:

$$\sum_{\rho,\lambda} q^{|\rho|} s_{\rho/\lambda}(x^{(1)}, x^{(2)}, \dots, x^{(N)}) s_{\rho/\lambda}(y^{(1)}, y^{(2)}, \dots, y^{(N)}) = \prod_{k=1}^{\infty} (1 - q^k)^{-1} \prod_{i,j=1}^{\infty} \left(1 - q^k x_i^{(1)} y_j^{(1)}\right)^{-1} \\ \prod_{i,j=1}^{\infty} \left(1 - q^k x_i^{(2)} y_j^{(1)}\right)^{-1} \dots \prod_{i,j=1}^{\infty} \left(1 - q^k x_i^{(1)} y_j^{(2)}\right)^{-1} \prod_{i,j=1}^{\infty} \left(1 - q^k x_i^{(2)} y_j^{(2)}\right)^{-1} \dots \prod_{i,j=1}^{\infty} \left(1 - q^k x_i^{(N)} y_j^{(M)}\right)^{-1}$$

where each of $x^{(j)}$ is an infinite series of variables $(x_1^{(j)}, x_2^{(j)}, x_3^{(j)}, \dots)$.

Using the fact that Schur functions are symmetric functions we can introduce the following variables and make use of the Eq.(8.8):

$$w_i = x_{\lfloor i/N \rfloor}^{(i \bmod N)} \\ z_i = y_{\lfloor i/M \rfloor}^{(i \bmod M)},$$

hence,

$$\sum_{\rho,\lambda} q^{|\rho|} s_{\rho/\lambda}(x^{(1)}, x^{(2)}, \dots, x^{(N)}) s_{\rho/\lambda}(y^{(1)}, y^{(2)}, \dots, y^{(N)}) = \sum_{\rho,\lambda} q^{|\rho|} s_{\rho/\lambda}(w) s_{\rho/\lambda}(z)$$

In these new variables the product will take the form

$$\prod_{i,j=1}^{\infty} (1 - q^k w_i z_j)^{-1} = \prod_{i=\{1,N+1,2N+1,\dots\}} \prod_{i=\{2,N+2,2N+2,\dots\}} \dots \prod_{j=1}^{\infty} (1 - q^k w_i z_j)^{-1} \\ = \prod_{i=\{1,N+1,2N+1,\dots\}} \prod_{j=1}^{\infty} (1 - q^k w_i z_j)^{-1} \prod_{i=\{2,N+2,2N+2,\dots\}} \prod_{j=1}^{\infty} (1 - q^k w_i z_j)^{-1} \dots \\ = \prod_{i=1}^{\infty} \prod_{j=1}^{\infty} (1 - q^k x_i^{(1)} z_j)^{-1} \prod_{i=1}^{\infty} \prod_{j=1}^{\infty} (1 - q^k x_i^{(2)} z_j)^{-1} \dots$$

The same approach as the above one for the product over j leads to the expression promised to be proved. For completeness, let us finish introducing some standard notation:

$$\kappa(\lambda) = 2 \sum_{(i,j) \in \lambda} (j - i) \tag{8.10}$$

$$\|\lambda\|^2 = \sum_i \lambda_i^2 \tag{8.11}$$

$$\kappa(\lambda) = \|\lambda\|^2 - \|\lambda^t\|^2 \tag{8.12}$$

⁷We pick one of these two similar forms, the other form is obvious and the proof is identical.

References

- [1] A. Iqbal, “All genus topological string amplitudes and 5-brane webs as Feynman diagrams,” hep-th/0207114.
- [2] M. Aganagic, A. Klemm, M. Marino, and C. Vafa, “The topological vertex,” *Commun. Math. Phys.* **254** (2005) 425–478, hep-th/0305132.
- [3] A. Borodin, “Periodic Schur process and cylindric partitions,” math/0601019.
- [4] A. Iqbal and C. Kozcaz, “U(N) Adjoint Theory, Cylindric Partitions and Hilbert Schemes,” work in progress.
- [5] E. Carlsson and A. Okounkov, “Exts and Vertex Operators,” arXiv.org:0801.2565.
- [6] S. Katz, P. Mayr, and C. Vafa, “Mirror symmetry and exact solution of 4D $N = 2$ gauge theories. I,” *Adv. Theor. Math. Phys.* **1** (1998) 53–114, hep-th/9706110.
- [7] A. Okounkov and N. Reshetikhin, “Random skew plane partitions and the Pearcey process,” math/0503508 [math.CO].
- [8] N. A. Nekrasov, “Seiberg-Witten prepotential from instanton counting,” *Adv. Theor. Math. Phys.* **7** (2004) 831–864, hep-th/0206161.
- [9] A. Iqbal, C. Kozcaz, and C. Vafa, “The Refined Topological Vertex,” *JHEP* **10** (2009) 069 hep-th/0701156.
- [10] A. Okounkov, N. Reshetikhin, and C. Vafa, “Quantum Calabi-Yau and classical crystals,” hep-th/0309208.
- [11] T. Okuda, “Derivation of Calabi-Yau crystals from Chern-Simons gauge theory,” *JHEP* **03** (2005) 047, hep-th/0409270.
- [12] P. Sulkowski, “Crystal model for the closed topological vertex geometry,” *JHEP* **12** (2006) 030, hep-th/0606055.
- [13] R. Donagi and E. Witten, “Supersymmetric Yang-Mills Theory And Integrable Systems,” *Nucl. Phys.* **B497**, 299 (1996) arXiv:hep-th/9510101.
- [14] E. Witten, “Solutions of four-dimensional field theories via M-theory,” *Nucl. Phys.* **B500**, 3 (1997) hep-th/9703166.
- [15] T. J. Hollowood, A. Iqbal, and C. Vafa, “Matrix Models, Geometric Engineering and Elliptic Genera,” hep-th/0310272.

- [16] K. A. Intriligator, D. R. Morrison, and N. Seiberg, “Five-dimensional supersymmetric gauge theories and degenerations of Calabi-Yau spaces,” *Nucl. Phys.* **B497** (1997) 56–100, hep-th/9702198.
- [17] I. G. Macdonald, “Symmetric functions and hall polynomials,” *Oxford Mathematical Monographs, Oxford Science Publications* (second edition, 1995).
- [18] N. Nekrasov and A. Okounkov, “Seiberg-Witten theory and random partitions,” hep-th/0306238.
- [19] S. Kerov, “Anisotropic Young diagrams and Jack symmetric functions,” arXiv:math/9712267.
- [20] I. Gessel and C. Krattenthaler, “Cylindric partitions,” *Trans. Amer. Math. Soc.* **349** (1997) no. 2, 429–479.
- [21] M. Haiman, “Notes on Macdonald polynomials and the geometry of Hilbert schemes,” *Symmetric Functions 2001: Surveys of Developments and Perspectives, Proceedings of the NATO Advanced Study Institute held in Cambridge, June 25-July 6, 2001, Sergey Fomin, editor. Kluwer, Dordrecht (2002), 1-64,*.
- [22] A. Iqbal, work in progress.